# Reliability considerations of modern design codes for CFST columns

Huu-Tai Thai[a,*], Son Thai[b], Tuan Ngo[a], Brian Uy[c], Won-Hee Kang[d], Stephen J. Hicks[e]

[a] Department of Infrastructure Engineering, The University of Melbourne, Parkville, VIC 3010, Australia

[b] Faculty of Civil Engineering, HCMC University of Technology, VNU-HCM, 268 Ly Thuong Kiet St, District 10, Ho Chi Minh City, Vietnam

[c] School of Civil Engineering, The University of Sydney, Sydney, NSW 2006, Australia

[d] Centre for Infrastructure Engineering, School of Engineering, Western Sydney University, Penrith, NSW 2751, Australia

[e] School of Engineering, The University of Warwick, Coventry, CV4 7AL, UK

**Abstract**

Concrete filled steel tubular (CFST) columns have been increasingly used in tall buildings and bridges due to offering excellent structural and economic benefits. Current design codes for such columns exhibit certain limits in terms of material strengths and section slenderness. This paper aims to evaluate the reliability and the applicability of the current design equations in American code AISC 360-16, European code EC 4 and Australian/New Zealand code ASNZS 2327 for the design of the columns beyond their material and slenderness limits. A comprehensive database with over 3,200 tests was collected to develop the statistics of the model errors for different types of columns. Monte Carlo and subset simulation techniques were developed based on Markov Chain Monte Carlo algorithms, to accurately and efficiently predict the reliability index of structures with small failure probability because they account for all uncertainties in material and geometric properties, loads and model errors. The results from the reliability analysis indicate that the reliability index of the concentric column designed by three considered codes is much higher than that of the eccentric column (i.e. beam-column). The results from a parametric study suggest that all three codes can be safely extended to the design of columns beyond the current material and section slenderness code limits.

*Keywords*: Design code; structural reliability; CFST column; test database

* Corresponding author. Tel.: +61 3 8344 6196
E-mail address: tai.thai@unimelb.edu.au (H.T. Thai)

## 1. Introduction

By employing the merits of both structural steel and concrete materials, CFST composite structures offer significant structural and economic benefits [1]. Therefore, they have been widely used in many civil engineering applications as a structural member under compression such as columns in tall buildings, towers in bridges and primary load-bearing members in large infrastructure [2]. Although the design guidelines for such columns have been given in many design codes and specifications (e.g., American code AISC 360-16 [3], European code EC 4 [4], British code BS 5400 [5], Chinese code GB 50936 [6], Japanese code AIJ [7] and Australian/New Zealand code ASNZS 2327 [8]), their design equations are only applicable to a certain limit of steel yield stress $f_y$ and concrete compressive strength $f'_c$. As shown in Table 1, most of the current design codes of practice are only applicable for CFST columns with normal strength steel and concrete, except for ASNZS 2327 [8] which allows for the use of high strength steel with $f_y$ up to 690 MPa and high strength concrete with $f'_c$ up to 100 MPa.

With recent breakthroughs in construction materials, ultra-high strength structural steel with $f_y$ from 690 MPa up to 1,300 MPa [9], and ultra-high strength concrete with $f'_c$ from 120 MPa up to 200 MPa [10] have become commercially available for use in modern construction. The use of high strength materials in composite construction not only reduces column sizes and consequently generates more valuable workspace for commercial use, but also provides sustainability benefits by reducing the use of construction materials. The practical use of ultra-high strength materials in modern composite construction is evidenced in the construction of Techno station (with $f_y$ of 780 MPa and $f'_c$ of 160 MPa) and a 38-storey office building (with $f_y$ of 780 MPa and $f'_c$ of 150 MPa [11]) in Tokyo, Japan. Therefore, in order to accommodate the use of such modern materials in composite construction, it is essentially important to assess the applicability of current design equations to CFST members beyond their material limits.

Extensive experimental study on high strength CFST columns has been carried out in recent years (see Refs. [12-33] and among others) to calibrate and evaluate the performance of current design equations beyond their material limits. Based on the test results of 146 CFST columns, Kilpatrick and Taylor [34] examined the applicability of EC 4 beyond its limits, and suggested that EC 4 can be reliably extended to high strength concrete with $f'_c$ up to 100 MPa. Goode and Lam [35] calibrated the design equations from EC 4 based on a test database with 1,819 specimens (including 1,808 tests on CFST columns) collected by Goode [36], and concluded that the EC 4 equations can be safety extended to CFST columns with $f'_c$ up to 100 MPa (for circular section) and 60 MPa (for square section). Liew et al. [37] also evaluated EC 4 design equations based on 2,033 test results, and concluded that the EC 4 method is applicable to high strength CFST columns with $f'_c$ up to 190 MPa and $f_y$ of 550 MPa. Tao et al. [38] evaluated the design equations given in Australian code AS 5100 based on a database of 2,194 columns. They found that the AS 5100 method gives similar results with the EC 4 approach, and thus it can be used for the design of high strength CFST columns. Leon et al. [39] collected experimental data from 2,213 tests on CFST columns to validate the AISC design equations. However, all these evaluations are based on a deterministic manner which ignores the statistics of geometric and material parameters.

To accurately assess the safety of a design code, reliability analyses should be used to evaluate the safety level in terms of the failure probability or the reliability index. The first-order reliability method (FORM) and Monte Carlo simulation (MCS) are the most commonly used reliability analysis methods to determine the reliability index. FORM is an approximate method which is only suitable for simple problems, whilst MCS is the most robust and accurate method which is suitable for complex problems with many random variables [40].

Whilst previous investigations on the reliability of CFST columns designed by existing codes of practice have been undertaken, the results from these studies are often limited due to the relatively small number of tests considered, or the form of the test specimens themselves.

For example, Sulyok and Galambos [41] and Lundberg and Galambos [42] evaluated the reliability of the design models given in EC4 [41] and AISC [42] using the FORM method. However, their study was based on only 226 test results of CFST columns, including 146 concentrically loaded columns and 80 eccentrically loaded columns. Beck et al. [43] assessed the reliability of American, Canadian, European and Brazilian codes using the FORM approach. Their study was based on only 93 experimental results, and limited to circular CFST columns under concentric loading. An et al. [44] evaluated the reliability of the design formulas given in American, European and Chinese codes using the FORM method. Their work was based on only 19 test columns, and limited to very slender CFST columns with normal strength materials. Lu et al. [45, 46] examined the reliability of American and European codes for CFST columns based on 100 experimental results of square columns [45] and 250 tests on circular columns [46], but their findings were limited to short columns under concentric loading. Recently, Thai and Thai [47] adopted the MCS approach to evaluate the safety level of EC 4 for the design of CFST columns. Their study was based on the largest number of tests with 2,224 test specimens. However, their study was limited to concentrically loaded columns.

To provide an accurate and comprehensive assessment of the safety level of current design codes for the design of CFST columns, this paper will collect the most up-to-date and comprehensive test database with 3,208 specimens collected from 184 references. The collected database covers a large range of material and geometric parameters of CFST columns which are well beyond the current code limits. Three design codes including American, European and Australian codes are considered in this study. The reliability index is calculated using the accurate direct MCS approach, which accounts for the error from the design models as well as the uncertainties in loadings, materials and geometry. A parametric study is also performed to explore the effect of design variables on the reliability index of the considered design codes.

## 2. Methodology

### *2.1 Overview of CFST test databases*

Since the CFST columns have been increasingly used in civil engineering applications, there have been significant efforts to compile comprehensive test databases of CFST columns for the calibration of the design equations currently used in design codes. The early work of this type was carried out by Aho [48] who collected 730 specimens of both encased and CFST columns tested mainly from the late 1990s and early 2000s. This database was later updated by Kim [49] with 451 new tests to make a new database with 1,181 specimens. Goode [36] also compiled another comprehensive database with 1,819 tests. This database was expanded by Tao et al. [38] with 2,194 specimens, Liew et al. [37] with 2,033 specimens and Thai et al. [1] with 3,103 specimens. Other comprehensive databases were also developed by Gourley et al. [50], Denavit [51] and Hajjar et al. [52] who provided detailed information of the experimental tests of not only CFST columns, but also other composite systems such as composite frames and composite beam-to-column connections.

The test database used in this study is expanded from our previous database [1] by adding over 100 tests (mainly high strength columns) published up to early 2020. Detailed properties and test results for each specimen of this database can be found in [53]. This is the most up-to-date and comprehensive database of CFST columns consisting of 3,208 specimens including 2,308 concentrically loaded columns (1,305 circular sections and 1,003 rectangular sections) and 900 eccentrically loaded columns (499 circular sections and 401 rectangular sections).

Table 2 summarises the range of geometric and material properties used in the test database and the limits of three codes considered in this study. The relative section slenderness is defined as $\lambda = (D/t)(f_y/E_s)$ for the circular section (with outside diameter $D$ and thickness $t$) and $\lambda = (b/t)\sqrt{f_y/E_s}$ for the rectangular section (with clear width $b$ and thickness $t$). The section slenderness limits given in EC 4 are converted as $\lambda_{\text{limit}} = 90\left(235/f_y\right)\left(f_y/E_s\right) = 0.11$ and $\lambda_{\text{limit}} = 52\sqrt{235/f_y} \times \sqrt{f_y/E_s} = 1.78$ for circular and rectangular sections, respectively. It is observed from Table 2 that the material and geometric properties used in the test database cover well beyond the current code limits, especially for $f'_c$.

The histogram distributions of the whole database versus the steel yield stress $f_y$, concrete strength $f'_c$, section slenderness $\lambda$ and member slenderness $\bar{\lambda}$ are also plotted in Fig. 1 with the code limits included for comparison purposes. It is worth noting that both AISC 360-16 and ASNZS 2327 have the same section slenderness limits (i.e., compact-to-noncompact, noncompact-to-slender and slender-to-permitted limits), and the term section slenderness limit used in this study refers to the maximum permitted limit. Since they allow for local buckling occurring in steel tubes, their section slenderness limit is much greater than that of EC 4, where the local buckling of steel tubes is restricted. The distribution and the number of tests within and beyond the code limits are plotted in Fig. 2 and summarised in Table 3 for different types of columns. It is found that a significant number of tests were conducted beyond the code limits. Among three considered codes, EC 4 allows the lowest limits of the section slenderness and material strengths. Therefore, it has the largest number of tests beyond its limits with 1,165 specimens (36.3%) beyond concrete strength limit and 725 specimens (22.6%) beyond section slenderness limit. If a combination of the limits for both section slenderness, steel and concrete materials is considered, the number of tests beyond the EC 4 limits is 1,746 specimens (54.4%) as shown in Table 3. This significant number of tests indicates that the current limits given in EC 4 are out-of-date and need to be extended. The corresponding numbers of tests beyond the limits of AISC 360-16 and ASNZS 2327 are only 28.7% and 11.8%, respectively.

*2.2 Design models*

Three modern codes of practice for the design of CFST columns are considered in this study including AISC 360-16, EC 4 and ASNZS 2327. The AISC 360-16 provisions do not allow the use of high strength materials, but do allow the use of slender sections. In AISC 360-16, the axial force-bending moment interaction equations have been modified from AISC 360-10 to account for the local buckling of beam-column members with noncompact and slender sections. Whereas, the use of CFST columns with slender sections is restricted in EC 4 [37]. The EC 4 design provisions are also limited to normal strength materials. An extension of EC 4 design guidelines to high strength materials was also developed by Liew and Xiong [54], and the second generation of this code is being prepared and will be published around 2024 [55]. ASNZS 2327 is the new Australian/New Zealand standard developed recently for steel-concrete composite structures in buildings [56, 57]. This is the only standard which allows for the use of both slender sections and high strength materials.

For the column under concentric loading, its section capacity is contributed from its steel tube and concrete infill. Unlike rectangular columns, the confining effect of the concrete core occurring in circular CFST columns will be significant, and thus it is taken into account in the design equations. In AISC 360-16 [3], the confining effect of the concrete core in circular CFST columns is included in compact sections via coefficient $C_2$ in Eq. (1) of the nominal section strength $P_{no}$.

$$P_{no} = A_s f_y + A_c C_2 f_c' \tag{1}$$

in which $A_s$ and $A_c$ are respectively the areas of steel and concrete. $C_2$ is increased from 0.85 (for reinforced concretes, steel-concrete composite beams and rectangular CFST columns) to 0.95 (for circular CFST columns). The local buckling effect of the steel tube of CFST columns with noncompact and slender sections is taken into account in AISC 360-16 [3] as shown in Fig. 3, where the nominal section strength is reduced nonlinearly as a function of the section slenderness $\lambda$ defined as $b/t$ (for rectangular section) or $D/t$ (for circular section) with $D$, $b$ and $t$ being the outside diameter of a circular section, the clear width of a rectangular section, and the thickness of a steel tube, respectively.

In EC 4 [4] and ASNZS 2327 [8], the confining effect of the concrete core in circular sections is taken into account in the same manner, in which $f'_c$ is increased by coefficient $\eta_c$ and $f_y$ is decreased by coefficient $\eta_s$ as illustrated in Eqs. (2) and (3) of the section strength $N_{us}$

$$N_{us}^{EC4} = A_s f_y \eta_s + A_c f'_c \left(1 + \eta_c \frac{t}{D} \frac{f_y}{f'_c}\right) \quad \text{from EC 4} \tag{2}$$

$$N_{us}^{AS} = k_f A_s f_y \eta_s + A_c f'_c \left(1 + \eta_c \frac{t}{D} \frac{f_y}{f'_c}\right) \quad \text{from ASNZS 2327} \tag{3}$$

The variations of the confining coefficients of the steel tube and concrete infill used in Eqs. (2) and (3) are illustrated in Fig. 4 for different steel sections. It is observed that the confining effect in concrete is more significant in compact sections and less pronounced in slender sections as expected due to local buckling of steel tubes. The confining effect is also more pronounced in short columns and negligibly small in long columns when the relative member slenderness $\bar{\lambda} = \sqrt{N_{us} / N_{cr}}$ (with $N_{us}$ and $N_{cr}$ being the section strength and Euler buckling load of the column, respectively) is greater than 0.5.

The values of elastic modulus of concrete and flexural stiffness of CFST columns are defined differently by three codes as illustrated in Table 4. It is worth noting that the local buckling of the steel tube which is ignored in EC 4 [4] is included in ASNZS 2327 [8] through the form factor $k_f$ in Eq. (3) by means of the effective width method. The form factor $k_f$ is equal to 1.0 for compact sections, and less than 1.0 for noncompact and slender sections to account for the local buckling effect. The member capacity is obtained by multiplying the section capacity with a reduction factor $\chi$ as shown in Fig. 5 to consider the global buckling effect. As shown in Fig. 5, the column curves of EC 4 and ASNZS 2327 (without local buckling effect, i.e. $k_f = 1$) are almost identical.

For the column under eccentric loading, its member capacity is calculated using the axial force $N$ and bending moment $M$ interaction diagram as shown in Fig. 6. AISC 360-16 allows two different methods to calculate the member strength of compact columns as shown in Fig. 6a. The first method (Method 1) is based on a bi-linear interaction curve as in the case of steel members, whilst the second method (Method 2) is based on a four-point interaction curve which is similar to that of EC 4 and ASNZS 2327. In Method 2, the interaction curve at the member level is developed by scaling down the axial force $N$ of the interaction curve at the section level by a slenderness reduction factor which is the ratio between the member and section strengths.

For the columns with noncompact and slender sections, the bi-linear interaction curve is modified as shown in Fig. 6a to account for the local buckling of the steel tubes. Both EC 4 and ASNZS 2327 adopt the four-point interaction curve as in the case of Method 2 of AISC 360-16, and use a similar procedure to account for initial member imperfections and second-order effects when deriving the interaction curve at the member level (the shaded part in Fig. 6b). In this procedure, the second-order moment due to initial member imperfection is assumed to vary linearly with the column axial force (the red line in Fig. 6b) starting from $\alpha_n$ to $\chi$ where $\alpha_n$ is taken as zero in EC4 and $\chi\left(1+\beta_m\right)/4$ in ASNZS 2327 with $\beta_m$ being the ratio of the smaller to the bigger end moments taken as a positive value when the member is bent in a reverse curvature. The effect of imperfections will be neglected when an axial load ratio is less than $\alpha_n$. For a column under concentric loading, its member strength indicated by $\chi$ is less than 1.0 due to the existence of the second-order moment $\mu_0$ caused by initial member imperfections. If an additional external moment is applied, the second-order moment caused by initial member imperfection is reduced from $\mu_0$ to $\mu_d$. Therefore, the available moment capacity at the member level is $\mu$ (the shaded part in Fig. 6b). Detailed calculations of the column strengths under eccentric loading for all three design codes can be found in our previous paper [1].

*2.3 Model error*

The strength predictions obtained from the design equations of the three considered codes are compared with the test results to calculate the statistics of the design model errors. In this comparison, all partial resistance factors of materials are taken as unity, and the measured values of material and geometric properties obtained from the test specimens are used. The distribution of the test-to-prediction ratios of all three codes are shown in Fig. 7 for columns and Fig. 8 for beam-columns. The results indicate that the mean value of the model error (i.e., test-to-prediction ratio) is slightly dependent on the slenderness $\bar{\lambda}$ of columns (see Fig. 7). However, for the case of beam-columns, the effect of the eccentricity on the mean model error is negligibly small (see Fig. 8), and thus it is ignored in this study. The statistical properties of the model errors of three considered codes obtained from a regression analysis are summarised in Table 5 for circular and rectangular columns and beam-columns.

The histograms of the test-to-prediction ratios are plotted in Figs. 9-11 for columns, beam-columns and all tests, respectively, with their statistics (coefficient of variation (CoV) and mean). Using a distribution fit tool in Matlab, it is found that all histograms are best fitted with a lognormal distribution. In general, all three codes predict the strength of rectangular columns slightly better than that of circular ones. However, the predictions of rectangular columns are less reliable and more scatter than those of circular ones due to with larger CoV (see Table 5). Both EC 4 and ASNZS 2327 give better predictions with less scatter compared with AISC 360-16 for both columns (see Fig. 9) and beam-columns (see Fig. 10).

For circular columns, the mean values $\mu$ predicted by EC 4 and ASNZS 2327 are only 1.095 and 1.079, respectively, which are lower than the values of 1.265 from AISC 360-16. This is due to the fact that both EC 4 and ASNZS 2327 adopt a more complex model to account for confining effect of concrete infill compared with the simple model used in AISC 360-16. Their confining model is based on more realistic confining behaviour which leads to an increase in concrete strength in addition to a reduction of steel yield stress due to local buckling effect as shown in Eqs. (2) and (3).

For the whole database (see Fig. 11), EC 4 provides the best predictions, whilst AISC 360-16 provides the most conservative predictions. Meanwhile, the accuracy of ASNZS 2327 is between those of EC 4 and AISC 360-16. This is expected, since ASNZS 2327 is a harmonised standard between EC 4 and AISC 360-16 which adopts the same confining model of EC 4 and the same section slenderness limit of AISC 360-16.

*2.4 Random variables*

To accurately predict the reliability index of the design codes, the uncertainty or randomness of all input variables including material, geometry and loads should be considered [58]. There are ten random variables considered in this study and their statistical properties are summarised in Table 6. For geometric properties, only the uncertainties in the cross-section of columns (i.e., thickness t of steel tubes, diameter D of circular sections or width B and height H of rectangular sections) are considered in this study. The uncertainty in the column length L is ignored because it is not sensitive to the reliability index of columns [42, 59, 60].

The statistics of geometric and material properties of steel tubes will be taken from [61, 62] whose input values are used in the next version of EC 3 on steel structures [63]. Meanwhile, the statistics of the concrete strength $f_c$' are based on those reported by Bartlett and Macgregor [64] (which are almost identical to the assumptions made in evaluating the partial factor for concrete within EC 2 [65]). The elastic modulus of concrete $E_c$ will be derived from $f_c$' using the design equations summarised in Table 4. The statistical distribution of geometric and material properties are assumed to be lognormal as recommended by the Joint Committee on Structural Safety (JCSS) Probabilistic Model Code [66] and Johnson and Huang [67]. This assumption was verified by Byfield and Nethercot [68] who proved that the lognormal distribution provides an accurate model of the lower tail of the probability distribution. There is no correlation between the geometric and material variables as demonstrated in [68]. The statistics of the model error (*ME* variable) are calculated based on the test database of 3,208 specimens collected in this study (see Table 5). As shown in Figs. 9 and 10, all distributions of the model errors are best fitted to lognormal types.

The statistical properties of dead load $D_n$ are obtained from Refs. [69, 70] with the characteristic value taken as the same as the mean value. For the live load $L_n$, two different approaches are adopted in the US code, European and Australian codes to calculate the characteristic value [71]. This might lead to the use of different values of the target reliability index (i.e., $\beta_T = 3.0$ in the US code and $\beta_T = 3.8$ in the European and Australian codes). In US practice, the characteristic value of the live load is defined as the mean value of the 50-year maxima based on Galambos [69] and Ellingwood [72] which appear to be the basis for the US loading standard ASCE/SEI 7 [73]. In European and Australian practice, the characteristic value of the live load is defined as the 98% fractile of the annual maximum loads [71] which results in a value of 0.6. This value is also recommended by JCSS and literature [70, 74, 75] which are the key references for the development of the European loading code [76] and Australian loading code [77]. In order to keep consistency with the loading standards, this study will adopt two different characteristic values of the live load $L_n$ for US code and European and Australian codes as shown in Table 6. It should be noted that the characteristic value used in previous studies [41, 43, 45-47] to evaluate the reliability of CFST columns designed according to EC 4 are based on the US practice instead of the European practice. Thus, their results cannot be compared directly with European requirements.

*2.5 Reliability analysis*

The safety level of structures designed following a given code can be measured by means of the reliability index $\beta$ related the failure probability $P_f$ as

$$\beta = -\Phi^{-1}\left(P_f\right) \tag{4}$$

where $\Phi$ is the standard cumulative distribution function. The failure probability $P_f$ can be predicted using either analytical approach or simulation method. Direct MCS approach can give accurate solutions for a problem with a large number of random variables as in the case of this study. In MCS, the failure probability can be calculated as

$$P_f = \frac{N_{fail}}{N} \tag{5}$$

where $N_{fail}$ and $N$ are the number of failed simulations (when the limit state function is violated, i.e. $g \leq 0$) and the total number of simulations, respectively; and $g$ is the limit state function of columns defined as

$$g = R - Q \tag{6}$$

where $R$ and $Q$ are the random values of column resistance and total design load, respectively, defined as

$$R = ME \times N_{uc} \tag{7}$$

$$Q = D_n + L_n \tag{8}$$

where $N_{uc}$ is the member resistance obtained from the design equations (see Section 2.2) using the random values of design variables given in Table 6 with the partial resistance factors taken as unity. The model error $ME$ is used to account for bias correction [42]. The nominal values $D_n$ and $L_n$ can be computed from the design resistance $N_{Rd}$ for a given $L_n/D_n$ as

$$D_n = \frac{N_{Rd}}{\gamma_D + \left(\frac{L_n}{D_n}\right)\gamma_L} \tag{9}$$

$$L_n = \left(\frac{L_n}{D_n}\right) D_n \tag{10}$$

where $N_{Rd}$ can be obtained from the design equations using the nominal values of material and geometric properties with the partial resistance factors included. The dead load $\gamma_D$ and live load $\gamma_L$ factors as well as the partial resistance factors of three considered codes are summarised in Table 7. The load factors for a combination of dead and live loads are taken from the US loading standard ASCE/SEI 7 [73], Eurocode 0 [78] and Australian/New Zealand loading standard

ASNZS 1170.1 [77]. A flowchart showing the step-by-step implementation of MCS is given in Fig. 12. The accuracy of MCS is dependent on the number of samples used in the simulation. The CoV of the probability of failure $P_f$ is related to the number of simulations $N$ as [79]

$$CoV = \sqrt{\frac{1-P_f}{NP_f}} \tag{11}$$

Eq. (11) indicates that the accuracy of MCS increases (smaller CoV) as the number of simulation $N$ increases. Table 8 shows the required number of samples $N$ and corresponding computational cost for different values of the reliability index $\beta$ to maintain the same level of accuracy with a CoV of 5%. It can be seen that a very large number of simulations $N$ is needed to handle the problem with a large reliability index $\beta$ or a small failure probability $P_f$ (from $2.96\times10^5$ to $4.05\times10^{11}$ samples for $\beta$ from 3.0 to 6.0).

Although the computational time for each simulation in this study is very efficient (about $10^5$ simulations per second with a laptop with normal configuration as shown in Table 8), the direct MCS is only applicable to the problem with a reliability index less than 4.5 (see Table 8). For small failure probability problem with a reliability index greater than 4.5, a subset simulation method [80-83] will be used to reduce computational time. The subset simulation is an adaptive simulation procedure developed by Au and Beck [80] based on the concept of conditional probability and Markov Chain Monte Carlo (MCMC) sampling techniques. Various MCMC algorithms have been proposed for subset simulation, and this study employs the adaptive conditional sampling approach proposed by Papaioannou et al. [81] as it significantly improves the performance of existing MCMC algorithms without increasing any computational cost [81].

Fig. 13 presents the results of MCS and subset simulation for a typical square stub column ($f_y$ = 300 MPa, $f'_c$ = 40 MPa, $t$ = 10 mm, $\lambda = 1.5$, $\overline{\lambda} = 0.2$) designed by ASNZS 2327. The MCS and subset results were obtained based on $5\times10^7$ and $10^5$ samples, respectively, to ensure the CoV of the estimated probability of failure $P_f$ less than 5%. It is also observed from Fig. 13b that the probability of failure predicted by the subset simulation method converges very fast with even a small number of samples (10,000 samples). Therefore, the subset simulation method is very efficient in predicting the reliability index of problems with very small failure probability.

## 3. Results and discussion

### *3.1 Reliability of columns designed by considered codes*

Based on the model errors given in Table 5, four different types of columns are categorised in this study including circular columns (CC), rectangular columns (RC), circular beam-columns (CB) and rectangular beam-columns (RB). For each type of column, a wide range of geometric and geometry parameters of column configurations is covered in the reliability analysis. They include seven values of steel yield stress $f_y$ = {200, 300, 400, 500, 600, 700, 800} MPa, seven values of concrete compressive strength $f'_c$ = {20, 30, 40, 60, 90, 120, 160} MPa, seven values of section slenderness ratio $\lambda = (D/t)(f_y/E_s)$ = {0.03, 0.05, 0.1, 0.15, 0.2, 0.25, 0.35} for circular sections or $\lambda = (b/t)\sqrt{f_y/E_s}$ = {1.0, 1.5, 2.0, 3.0, 4.0, 5.0, 6.0} for rectangular sections, and seven values for the member slenderness ratio $\bar{\lambda} = \sqrt{N_{us}/N_{cr}}$ = {0.15, 0.3, 0.5, 1.0, 1.5, 2.0, 2.5}. As shown in Fig. 1, these values reflect the wide range of column configurations covered by the test database, and thus the reliability indices of the columns with section and material properties beyond the code limits can be addressed. . In total, there are 7×7×7×7 = 2,401 column configurations considered for a single category of columns. With four different column categories and three considered codes, the total number of reliability problems simulated is 4×3×2,401 = 28,812. A typical value of live load-to-dead load ratio $L_n/D_n$ of 1.0 was used as most of structures have $L_n/D_n \leq 2.0$ [84]. For beam-columns, the eccentricity $e$ is taken as 0.05×$D$ to ensure the confining effect is taken into account in the equations of EC 4 and ASNZS 2327.

Table 9 summarises the reliability indices of the full range of column configurations designed by the three considered codes. Since the reliability varies in different column configurations, the statistical properties of the obtained reliability index (i.e., minimum value, maximum value, mean value and CoV) are summarised for comparison purposes. It should be noted that the mean values of the reliability indices of the columns designed by EC 4 obtained in this study are much greater than those predicted in existing studies (e.g., $\beta$ =2.3 – 2.5 [42], 2.9 [43] and 3.2 [45]). This is mainly due to the use of the characteristic values of live load of 0.6 [70, 74, 75] (see Table 6) which is smaller than the mean value of 1.0 adopted in existing studies based on the practice of American code calibrations. In general, the reliability indices of concentric columns designed by three considered codes are higher than those of eccentric columns (i.e., beam-columns). This is because the prediction models of columns are better than those of beam-columns with less scatter and smaller CoV as shown in Fig. 9 (for concentric columns) and Fig. 10 (for eccentric columns).

It can be seen from Table 9 that the minimum values of the reliability index of concentric columns designed by AISC 360-16 are above the target reliability index $\beta_T$ of 3.0 required by American code for a column under a dead load and live load combination [85]. This is also observed for the concentric columns with section and material properties beyond the AISC 360-16 code limits. The mean value of the obtained reliability index is about 20% - 30% higher than the target value. This means that the design equations of CFST columns in AISC 360-16 code can be safely extended beyond the current limits. However, this is not the case for eccentric columns (i.e., CB and RB). Although their mean values narrowly meet the target requirement, their minimum values are still lower than the target values of 3.0. It is interesting to note from Table 9 that the reliability indices of the column configurations beyond the AISC 360-16 code limits are more uniform (less scatter and smaller CoV) than those of the column configurations within the code limits.

As shown in Table 9, both EC 4 and ASNZS 2327 give a similar safety level for circular concentric columns (CC) with the reliability indices being in the range from 3.9 to 5.3 for EC 4 (or 3.8 to 5.2 for ASNZS 2327). These values are well above the target value $\beta_T$ of 3.8 recommended by EC 0 [78] and AS 5104 [86] (adopted from ISO 2394 [87]) for the design of members of a Class 2 structure (office and residential buildings) with the probability of failure of 1 in 14,000 over a reference period of 50 years). Although the mean value of the reliability index of the RC designed by EC 4 and ASNZS 2327 is around 4.0, which meets the target value of 3.8, its minimum value is 3.5 which falls slightly below the required target value of 3.8. Similar to the eccentric column designed by AISC 360-16, the reliability index of the eccentric column designed by EC 4 and ASNZS 2327 is smaller than that of concentric columns, and its mean values are also lower than the target value of 3.8. Table 9 also indicates that both the ASNZS 2327 and EC 4 design models can be extended to the column configurations beyond the current material and section slenderness limits, since the reliability indices of columns within and beyond the code limits are almost identical.

*3.2 Effect of design variables*

In order to accurately assess the reliability of a design code beyond its current material and slenderness limits, a parametric study was performed for a wide range of material and geometric parameters including those within and beyond the code limits. Three main variables considered in this study include $f_y$, $f_c$' and $\lambda$. Figs. 14 and 15 show the effects of $f_y$ and $f_c$' on the reliability index of the three considered codes, respectively. In this parametric study, all geometric and loading properties, except for $f_y$ and $f_c$', are kept the same with those of the typical columns ($f_y$ = 300 MPa, $f'_c$ = 40 MPa, $t$ = 10 mm, $\lambda = 1.5$ (rectangular section) and 0.05 (circular section), $\bar{\lambda} = 0.2$). The steel yield stress $f_y$ is varied from 100 MPa to 1,000 MPa, whilst $f_c$' is varied from 10 MPa to 200 MPa. In order to ensure the compatibility between concrete and steel materials in a CFST section (i.e., to avoid the crushing of the concrete infill before the yielding of the steel tube), the selection of steel grade $f_y$ should be matched with concrete grade $f_c$' based on the following condition [54]

$$f_y \leq 0.7E_s\left(f_c^{'}+8\right)^{0.31} \tag{12}$$

In general, the reliability indices obtained from the three considered codes are insensitive to both $f_y$ and $f_c$', and they also exceed the target reliability $\beta_T$ for all column types designed by AISC 360-16 with material strengths within and beyond the current code limits. It means that they can be safety extended to the design of high strength CFST columns with $f_y$ up to 1,000 MPa (see Fig. 14) and $f_c$' up to 200 MPa (see Fig. 15). For the column designed by EC 4 and ASNZS 2327, its reliability index is slightly decreased by increasing the steel yield stress.

Fig. 16 shows the variation of the reliability index with respect to the section slenderness ratio of columns. In this case study, except for section slenderness ratio, all geometric, material and loading properties are kept the same as in the case of the typical columns. In general, the reliability index of the column designed by AISC 360-16 slightly decreased with the increase of the section slenderness ratio especially the region within the code limit. This tendency is somehow opposite for the column designed by EC 4 and ASNZS 2327. Fig. 16c also indicates that ASNZS 2327 can be safety extended to the design all column configurations with the section slenderness ratio beyond the current code limits.

The last case study is to investigate the effect $L_n/D_n$ on the reliability index of the CFST columns designed by the three considered codes. The variation of the reliability index with respect to $L_n/D_n$ is shown in Fig. 17 when all geometric and material properties are kept the same with those of the typical columns. It is observed that the reliability index of the columns design by three considered codes are only sensitive to cases when the live load-to-dead load ratio $L_n/D_n$ is less than 1.0.

## 4. Conclusions

This study evaluates the reliability of the CFST columns designed by AISC 360-16, EC 4 and ASNZS 2327, and examines whether the existing design rules can be extended to columns with material strengths and section slenderness ratios beyond the current code limits. A comprehensive test database with 3,208 columns (including 656 circular stub columns, 649 circular long columns, 499 circular beam-columns, 572 rectangular stub columns, 431 rectangular long columns, and 401 rectangular beam-columns) was collected to develop the statistical parameters of the model errors for the three considered codes. To the present authors knowledge, this is the first time that the statistics of model errors for CFST columns have been developed for AISC 360-16, EC 4 and ASNZS 2327 based on the most up-to-date database collected in this study. The statistics of model error are then included in the direct MCS or subset simulation which accounts for the uncertainties in materials, geometry and loads to accurately predict the reliability index. The following findings are obtained from this study:

(1) A significant number of tests collected in this study have the material strengths and section slenderness ratios beyond the current code limits. Among three considered codes, EC 4 has the largest number of tests beyond its limits with 1,746 specimens (54.4%). The corresponding numbers of tests beyond the limits of AISC 360-16 and ASNZS 2327 are 912 specimens (28.7%) and 379 specimens (11.8%), respectively. This finding implies that the current limits in EC 4 are out-of-date and need to be extended.

(2) Among the three considered codes, AISC 360-16 provides the most conservative predictions, especially for circular columns where the confining effect existed. Whereas, both EC 4 and ASNZS 2327 provide more accurate predictions with smaller means and CoVs compared with the predictions obtained from AISC 360-16. This is due to the fact that the design equations given by EC 4 and ASNZS 2327 are more complex and are based on a more realistic behaviour than the simple equations given in AISC 360-16. All

histograms of model error fitted well with a lognormal distribution.

(3) In general, the reliability index of the concentric columns designed by the three considered codes are higher than that of eccentric columns.

(4) The results from the reliability analysis also indicate that all three considered codes can be extended to the design of CFST columns with material strengths and section slenderness beyond their current code limits as the reliability indices of column configurations within and beyond the code limits are almost identical.

**Acknowledgements**

This research was supported by the Australian Research Council (ARC) under its Future Fellowship Scheme (Project No: FT200100024), and the University of Melbourne under a Start-up Grant awarded to the first author. The financial support is gratefully acknowledged.

**References**

[1] Thai S, Thai H-T, Uy B, Ngo T. Concrete-filled steel tubular columns: Test database, design and calibration. Journal of Constructional Steel Research 2019;157:161-181.

[2] Han L-H, Li W, Bjorhovde R. Developments and advanced applications of concrete-filled steel tubular (CFST) structures: Members. Journal of Constructional Steel Research 2014;100:211-228.

[3] AISC 360-16. Specification for structural steel buildings; 2016.

[4] EN1994-1-1. Eurocode 4: Design of composite steel and concrete structures - Part 1-1: General rules and rules for buildings; 2004.

[5] BS5400-5. Steel, concrete and composite bridges. Code of practice for design of composite bridges. British Standards Institute (BSI); 2005.

[6] GB 50936. Technical code for concrete-filled steel tubular structures. China National Standards; 2014.

[7] Architectural Institute of Japan (AIJ). Recommendations for design and construction of

concrete filled steel tubular structures, Japan; 1997.

[8] Standards Australia. AS/NZS 2327 Composite structures - Composite steel-concrete construction in buildings; 2017.

[9] STRENX. Strenx 1300 - The ultra-high-strength steel at 1300 MPa, from https://www.ssab.com/products/brands/strenx/products/strenx-1300; 2020.

[10] Azmee NM, Shafiq N. Ultra-high performance concrete: From fundamental to applications. Case Studies in Construction Materials 2018;9:e00197.

[11] Matsumoto S, Hosozawa O, Narihara H, Komuro T, Kawamoto S-i. Structural design of an ultra high-rise building using concrete filled tubular column with 780 MPa class high-strength steel and 150 MPa high-strength concrete. International Journal of High-Rise Buildings 2014;3:73-79.

[12] Song T-Y, Xiang K. Performance of axially-loaded concrete-filled steel tubular circular columns using ultra-high strength concrete. Structures 2020;24:163-176.

[13] Xiong M-X, Liew JYR, Wang Y-B, Xiong D-X, Lai B-L. Effects of coarse aggregates on physical and mechanical properties of C170/185 ultra-high strength concrete and compressive behaviour of CFST columns. Construction and Building Materials 2020;240:117967.

[14] Wang J, Sun Q, Li J. Experimental study on seismic behavior of high-strength circular concrete-filled thin-walled steel tubular columns. Engineering Structures 2019;182:403-415.

[15] Lee H-J, Park H-G, Choi I-R. Compression loading test for concrete-filled tubular columns with high-strength steel slender section. Journal of Constructional Steel Research 2019;159:507-520.

[16] Hoang AL, Fehling E, Lai B, Thai DK, Chau NV. Experimental study on structural performance of UHPC and UHPFRC columns confined with steel tube. Engineering

Structures 2019;187:457-477.

[17] Huang Z, Li D, Uy B, Thai H-T, Hou C. Local and post-local buckling of fabricated high-strength steel and composite columns. Journal of Constructional Steel Research 2019;154:235-249.

[18] Li D, Huang Z, Uy B, Thai H-T, Hou C. Slenderness limits for fabricated S960 ultra-high-strength steel and composite columns. Journal of Constructional Steel Research 2019;159:109-121.

[19] Lee H-J, Park H-G, Choi I-R. Eccentric compression behavior of concrete-encased-and-filled steel tube columns with high-strength circular steel tube. Thin-Walled Structures 2019;144:106339.

[20] Patel VI, Hassanein MF, Thai H-T, Al Abadi H, Elchalakani M, Bai Y. Ultra-high strength circular short CFST columns: Axisymmetric analysis, behaviour and design. Engineering Structures 2019;179:268-283.

[21] Li G, Chen B, Yang Z, Feng Y. Experimental and numerical behaviour of eccentrically loaded high strength concrete filled high strength square steel tube stub columns. Thin-Walled Structures 2018;127:483-499.

[22] Hassanein MF, Patel VI, Elchalakani M, Thai H-T. Finite element analysis of large diameter high strength octagonal CFST short columns. Thin-Walled Structures 2018;123:467-482.

[23] Xiong M-X, Xiong D-X, Liew JYR. Axial performance of short concrete filled steel tubes with high- and ultra-high- strength materials. Engineering Structures 2017;136:494-510.

[24] Du Y, Chen Z, Richard Liew JY, Xiong M-X. Rectangular concrete-filled steel tubular beam-columns using high-strength steel: Experiments and design. Journal of Constructional Steel Research 2017;131:1-18.

[25] Du Y, Chen Z, Wang Y-B, Richard Liew JY. Ultimate resistance behavior of rectangular

concrete-filled tubular beam-columns made of high-strength steel. Journal of Constructional Steel Research 2017;133:418-433.

[26] Khan M, Uy B, Tao Z, Mashiri F. Concentrically loaded slender square hollow and composite columns incorporating high strength properties. Engineering Structures 2017;131:69-89.

[27] Xiong M-X, Xiong D-X, Liew JYR. Behaviour of steel tubular members infilled with ultra high strength concrete. Journal of Constructional Steel Research 2017;138:168-183.

[28] Xiong M-X, Xiong D-X, Liew JYR. Flexural performance of concrete filled tubes with high tensile steel and ultra-high strength concrete. Journal of Constructional Steel Research 2017;132:191-202.

[29] Khan M, Uy B, Tao Z, Mashiri F. Behaviour and design of short high-strength steel welded box and concrete-filled tube (CFT) sections. Engineering Structures 2017;147:458-472.

[30] Zarringol M, Thai H-T, Ngo T, Patel V. Behaviour and design calculations of rectangular CFST beam-columns with slender sections. Engineering Structures 2020;222:111142.

[31] Phan DHH, Patel VI, Al Abadi H, Thai H-T. Analysis and design of eccentrically compressed ultra-high-strength slender CFST circular columns. Structures 2020;27:2481-2499.

[32] Thai H-T, Uy B, Khan M. A modified stress-strain model accounting for the local buckling of thin-walled stub columns under axial compression. Journal of Constructional Steel Research 2015;111:57-69.

[33] Thai H-T, Uy B, Khan M, Tao Z, Mashiri F. Numerical modelling of concrete-filled steel box columns incorporating high strength materials. Journal of Constructional Steel Research 2014;102:256-265.

[34] Kilpatrick A, Taylor T. Application of Eurocode 4 design provisions to high strength composite columns. IABSE Reports 1997:561-566.

[35] Goode CD, Lam D. Concrete-filled steel tube columns - tests compared with Eurocode 4. Proceeding of Composite Construction in Steel and Concrete VI in Colorado, USA 2008.

[36] Goode CD. Composite columns - 1819 tests on concrete-filled steel tube columns compared with Eurocode 4. The Institution of Structural Engineers 2008;86:33-38.

[37] Liew JYR, Xiong M, Xiong D. Design of concrete filled tubular beam-columns with high strength steel and concrete. Structures 2016;8:213-226.

[38] Tao Z, Brian UY, Han LH, He SH. Design of concrete-filled steel tubular members according to the Australian standard as 5100 model and calibration. Australian Journal of Structural Engineering 2008;8:197-214.

[39] Leon RT, Perea T, Hajjar JF, Denavit MD. Concrete-filled tubes columns and beam-columns: A database for the AISC 2005 and 2010 specifications. Festschrift Gerhard Hanswille, Germany 2011:203-212.

[40] Thai H-T, Uy B, Kang W-H, Hicks S. System reliability evaluation of steel frames with semi-rigid connections. Journal of Constructional Steel Research 2016;121:29-39.

[41] Sulyok M, Galambos TV. Reliability of composite columns and beam-columns in Eurocode 4. International Journal of Engineering Modelling 1994;7:2.

[42] Lundberg JE, Galambos TV. Load and resistance factor design of composite columns. Structural safety 1996;18:169-177.

[43] Beck AT, de Oliveira WLA, De Nardim S, ElDebs ALHC. Reliability-based evaluation of design code provisions for circular concrete-filled steel columns. Engineering Structures 2009;31:2299-2308.

[44] An Y-F, Han L-H, Zhao X-L. Behaviour and design calculations on very slender thin-walled CFST columns. Thin-Walled Structures 2012;53:161-175.

[45] Lu Z-H, Zhao Y-G, Yu Z, Chen C. Reliability-based assessment of American and European specifications for square CFT stub columns. Steel and Composite Structures 2015;19:811-

827.

[46] Lu Z-H, Zhao Y-G, Yu Z-W, Xu Q-Y. Reliability-based assessment of design code provisions for circular CFT stub columns. Advances in Structural Engineering 2012;15:1921-1933.

[47] Thai H-T, Thai S. Reliability evaluation of Eurocode 4 for concrete-filled steel tubular columns. Paper presented at: CIGOS 2019, Innovation for Sustainable Infrastructure, 2020; Ha Noi, Vietnam.

[48] Aho MK. A database for encased and concrete-filled columns. Master thesis, School of Civil and Environmental Engineering, Georgia Institute of Technology 1996.

[49] Kim DK. A database for composite columns. Master thesis, School of Civil and Environmental Engineering, Georgia Institute of Technology 2005.

[50] Gourley BC, Tort C, Denavit MD, Schiller PH, Hajjar JF. A synopsis of studies of the monotonic and cyclic behavior of concrete-filled steel tube members, connections, and frames. Department of Civil and Environmental Engineering, University of Illinois at Urbana-Champaign 2008.

[51] Denavit M. Steel-concrete composite column database, from http://mark.denavit.me/Composite-Column-Database; 2019.

[52] Hajjar JF, Gourley BC, Tort C, Denavit MD, Schiller PH. Steel-concrete composite structural systems. Department of Civil and Environmental Engineering, Northeastern University, Boston, Massachusetts, <http://www.northeastern.edu/compositesystems> 2019.

[53] Thai S, Thai H-T, Uy B, Ngo T, Naser MZ. Test database on concrete-filled steel tubular columns. Mendeley Data 2019;DOI: 10.17632/3xknb3sdb5.2.

[54] Liew JR, Xiong M. Design guide for concrete filled tubular members with high strength materials - an extension of Eurocode 4 method to C90/105 concrete and S550 steel:

Research Publishing; 2015.

[55] Schafer M. European design code for composite structures in steel and concrete. Steel Construction 2019;12:70-81.

[56] Hicks SJ, Uy B. AS/NZS 2327 Composite structures: A new standard for steel-concrete composite buildings. Proceedings of the Steel Innovations Conference, Auckland, New Zealand 2015:8.

[57] Uy B, Hicks SJ, Kang W-H, Thai H-T, Aslani F. The new Australia/New Zealand standard on composite steel-concrete buildings. Proceedings of the 8th International Conference on Composite Construction in Steel and Concrete, Wyoming, United States 2018.

[58] Hess PE, Bruchman D, Assakkaf IA, Ayyub BM. Uncertainties in material and geometric strength and load variables. Naval Engineers Journal 2002;114:139-166.

[59] Zarringol M, Thai H-T, Thai S, Patel V. Application of ANN to the design of CFST columns. Structures 2020;28:2203-2220.

[60] Naser MZ, Thai S, Thai H-T. Evaluating structural response of concrete-filled steel tubular columns through machine learning. Journal of Building Engineering 2020:101888.

[61] European Commission. Standardization of Safety Assessment Procedures across Brittle to Ductile Failure Modes (SAFEBRICTILE): Publications Office of the European Union, Luxembourg; 2017.

[62] Knobloch M, Bureau A, Kuhlmann U, da Silva LS, Snijder HH, Taras A, et al. Structural member stability verification in the new Part 1-1 of the second generation of Eurocode 3. Steel Construction 2020;13:98-113.

[63] prEN 1993-1-1:2020. Eurocode 3: Design of steel structures - Part 1-1: General rules and rules for buildings (https://standardsdevelopment.bsigroup.com/categories/91.010.30, accessed 17/10/20); 2020.

[64] Bartlett FM, Macgregor JG. Statistical analysis of the compressive strength of concrete in

structures. ACI Materials Journal 1996;93:158-168.

[65] European Concrete Platform. Eurocode 2 Commentary, https://www.theconcreteinitiative.eu/images/ECP_Documents/Eurocode2_Commentary.pdf; 2017.

[66] JCSS. Probabilistic Model Code. Part III - Resistance models 2001.

[67] Johnson RP, Huang D. Calibration of safety factors γm for composite steel and concrete beams in bending. Proceedings of the Institution of Civil Engineers - Structures and Buildings 1994;104:193-203.

[68] Byfield MP, Nethercot DA. Material and geometric properties of structural steel for use in design. The Structural Engineer 1997;75:363-367.

[69] Galambos TV. Load and resistance factor design. Engineering Journal, AISC 1981;18:74-82.

[70] European Commission. Development of skills facilitating implementation of Eurocodes. Handbook 2 - Reliability backgrounds: The Leonardo da Vinci Pilot Project CZ/02/B/F/PP-134007; 2005.

[71] Honfi D. Serviceability floor loads. Structural Safety 2014;50:27-38.

[72] Ellingwood BR. Probability-based LRFD for engineered wood construction. Structural Safety 1997;19:53-65.

[73] ASCE/SEI 7-10. Minimum design loads for buildings and other structures; 2010.

[74] Markova J, Sousa ML, Dimova S, Athanasopoulou A, Iannaccone S. Reliability of structural members designed with the Eurocodes NDPs selected by EU and EFTA Member States. EUR 29410 EN, Publications Office of the European Union, Luxembourg, 2018, ISBN 978-92-79-96815-0, doi:10.2760/426349, JRC113687; 2018.

[75] Gulvanessian H, Holicky M. Eurocodes: using reliability analysis to combine action effects. Proceedings of the Institution of Civil Engineers - Structures and Buildings

2005;158:243-252.

[76] EN1991-1-1. Eurocode 1: Actions on structures - Part 1-1: General actions - Densities, self-weight, imposed loads for buildings; 2002.

[77] Standards Australia. ASNZS 1170.1 Structural design actions - Part 1: Permanent, imposed and other actions; 2002.

[78] EN1990. Eurocode 0: Basis of structural design; 2002.

[79] Soong TT, Grigoriu M. Random vibration of mechanical and structural systems: Prentice Hall; 1993.

[80] Au S-K, Beck JL. Estimation of small failure probabilities in high dimensions by subset simulation. Probabilistic Engineering Mechanics 2001;16:263-277.

[81] Papaioannou I, Betz W, Zwirglmaier K, Straub D. MCMC algorithms for Subset Simulation. Probabilistic Engineering Mechanics 2015;41:89-103.

[82] Li H-S, Cao Z-J. Matlab codes of Subset Simulation for reliability analysis and structural optimization. Structural and Multidisciplinary Optimization 2016;54:391-410.

[83] Vrugt JA. Markov chain Monte Carlo simulation using the DREAM software package: Theory, concepts, and MATLAB implementation. Environmental Modelling & Software 2016;75:273-316.

[84] Ellingwood B, Galambos TV, MacGregor JG, Cornell CA. Development of a probability based load criterion for american national standard a58: National Bureau of Standards Special Publication 577: U.S. Government Printing Office, Washington DC; 1980.

[85] Ellingwood B, Galambos TV. Probability-based criteria for structural design. Structural Safety 1982;1:15-26.

[86] Standards Australia. AS 5104 General principles on reliability for structures; 2017.

[87] International Organization for Standardization. ISO 2394 General principles on reliability for structures; 2015.

Table 1. Material limits in modern codes of practice

| Design codes | Steel yield stress (MPa) | Concrete compressive strength (MPa) |
|---|---|---|
| AISC 360-16 [3] | 525 | 69 |
| EC 4 [4] | 460 | 50 |
| BS 5400 [5] | 460 | 50 |
| GB 50936 [6] | 420 | 70* |
| AIJ [7] | 440 | 90 |
| ASNZS 2327 [8] | 690 | 100 |

* This value refers to the compressive strength from cube specimens.

Table 2. Range of material and geometry properties used in the test database and code limits

| Properties | | Min | Max | Code limits | | |
|---|---|---|---|---|---|---|
| | | | | EC 4 | AISC 360-16 | ASNZS 2327 |
| Steel yield stress, $f_y$ (MPa) | | 115.00 | 853.00 | 460 | 525 | 690 |
| Concrete strength, $f_c$' (MPa) | | 7.59 | 185.94 | 50 | 69 | 100 |
| Section slenderness | Circular section | 0.01 | 0.26 | 0.11 | 0.31 | 0.31 |
| | Rectangular section | 0.05 | 9.93 | 1.78 | 5.0 | 5.0 |
| Member slenderness | Circular section, $L/D$ | 0.81 | 51.48 | | | |
| | Rectangular section, $L/B$ | 0.59 | 49.10 | | | |

Table 3. Summary of the test database

| Types of column | EC 4 | AISC 360-16 | ASNZS 2327 |
|---|---|---|---|
| Circular short column (656 tests) | | | |
| No. of test with $f_y$ beyond code limits | 39 (5.9%)* | 24 (3.7%) | 12 (1.8%) |
| No. of test with $f'_c$ beyond code limits | 302 (46.0%) | 240 (36.6%) | 91 (13.9%) |
| No. of test with $\lambda$ beyond code limits | 152 (23.2%) | 0 | 0 |
| Circular long column (649 tests) | | | |
| No. of test with $f_y$ beyond code limits | 54 (8.3%) | 17 (2.6%) | 0 |
| No. of test with $f'_c$ beyond code limits | 89 (13.7%) | 47 (7.2%) | 25 (3.8%) |
| No. of test with $\lambda$ beyond code limits | 56 (8.6%) | 0 | 0 |
| Circular beam-column (499 tests) | | | |
| No. of test with $f_y$ beyond code limits | 12 (2.4%) | 0 | 0 |
| No. of test with $f'_c$ beyond code limits | 206 (41.3%) | 76 (15.2%) | 25 (5.0%) |
| No. of test with $\lambda$ beyond code limits | 38 (7.6%) | 0 | 0 |
| Rectangular short column (572 tests) | | | |
| No. of test with $f_y$ beyond code limits | 167 (29.2%) | 137 (23.9%) | 87 (15.2%) |
| No. of test with $f'_c$ beyond code limits | 232 (40.5%) | 164 (28.7%) | 68 (11.9%) |
| No. of test with $\lambda$ beyond code limits | 194 (33.9%) | 5 (0.9%) | 5 (0.9%) |
| Rectangular long column (431 tests) | | | |
| No. of test with $f_y$ beyond code limits | 88 (20.4%) | 61 (14.1%) | 45 (10.4%) |
| No. of test with $f'_c$ beyond code limits | 163 (37.8%) | 96 (22.3%) | 55 (12.8%) |
| No. of test with $\lambda$ beyond code limits | 156 (36.2%) | 6 (1.4%) | 6 (1.4%) |
| Rectangular beam-column (401 tests) | | | |
| No. of test with $f_y$ beyond code limits | 89 (22.2%) | 55 (13.7%) | 21 (5.2%) |
| No. of test with $f'_c$ beyond code limits | 173 (43.1%) | 115 (28.7%) | 12 (3.0%) |
| No. of test with $\lambda$ beyond code limits | 129 (19.7%) | 0 | 0 |
| All test data (3,208 tests) | | | |
| No. of test with $f_y$ beyond code limits | 449 (14.0%) | 294 (9.2%) | 165 (5.1%) |
| No. of test with $f'_c$ beyond code limits | 1165 (36.3%) | 738 (23.0%) | 276 (8.6%) |
| No. of test with $\lambda$ beyond code limits | 725 (22.6%) | 11 (0.3%) | 11 (0.3%) |
| All test data (3,208 tests) | | | |
| No. of test within code limits | 1,462 (45.6%) | 2,287 (71.3%) | 2,829 (88.2%) |
| No. of test beyond code limits | 1,746 (54.4%) | 912 (28.7%) | 379 (11.8%) |

* The value in bracket indicates the corresponding percentage.

Table 4. Recommended elastic modulus of concrete and flexural stiffness of CFST columns

| Design codes | Elastic modulus $E_c$ | Flexural stiffness $EI$ |
| --- | --- | --- |
| AISC 360-16 [3] | $E_c = 0.043\rho^{1.5}\sqrt{f_c'}$ | $EI = E_s I_s + C_3 E_c I_c$ where $C_3 = 0.45 + 3\dfrac{A_s}{A_s + A_c} \le 0.9$ |
| EC 4 [4] | $E_c = 22\left[(f_c' + 8)/10\right]^{0.3}$ | $EI = E_s I_s + 0.6 E_c I_c$ |
| ASNZS 2327 [8] | $E_c = \begin{cases} \rho^{1.5} 0.043\sqrt{f_{cmi}} & \text{if } f_{cmi} \le 40MPa \\ \rho^{1.5}\left(0.024\sqrt{f_{cmi}} + 0.12\right) & \text{if } f_{cmi} > 40MPa \end{cases}$ where $f_{cmi} = 0.9\left(1.2875 - 0.001875 f_c'\right) f_c'$ | $EI = E_s I_s + E_c I_c$ |

$\rho$ is the density of concrete and can be taken as 2,400 kg/m$^3$.

Table 5. Statistical properties of model errors based on regressive analysis

| Type of column | Type of section | No. of tests (n) | Code | Mean ($\mu$) | CoV |
| --- | --- | --- | --- | --- | --- |
| Column | Circular | 1305 | AISC 360-16 | $0.0248/\bar{\lambda} + 1.134$ | 0.157 |
| | | | EC 4 | $0.179\bar{\lambda} + 1.033$ | 0.142 |
| | | | ASNZS 2327 | $0.101\bar{\lambda} + 1.042$ | 0.135 |
| | Rectangular | 1003 | AISC 360-16 | $0.0009\bar{\lambda} + 1.165$ | 0.171 |
| | | | EC 4 | $0.169\bar{\lambda} + 1.012$ | 0.172 |
| | | | ASNZS 2327 | $0.0856\bar{\lambda} + 1.044$ | 0.161 |
| Beam-column | Circular | 499 | AISC 360-16 | 1.245 | 0.250 |
| | | | EC 4 | 1.115 | 0.193 |
| | | | ASNZS 2327 | 1.187 | 0.200 |
| | Rectangular | 401 | AISC 360-16 | 1.221 | 0.235 |
| | | | EC 4 | 1.061 | 0.194 |
| | | | ASNZS 2327 | 1.107 | 0.189 |

Note: All histograms are best fitted to a lognormal distribution.

Table 6. Statistical properties of random variables

| Properties | Variables | Mean | CoV | Distribution | Reference |
|---|---|---|---|---|---|
| Material | X(1) = Elastic modulus of steel, $E_s$ | 1.00 | 0.030 | Lognormal | [61, 62] |
| | X(2) = Steel yield stress, $f_y$ < 355 MPa | 1.25 | 0.055 | Lognormal | [61, 62] |
| | $f_y$ < 420 MPa | 1.20 | 0.050 | | |
| | $f_y$ < 460 MPa | 1.15 | 0.045 | | |
| | $f_y \geq$ 460 MPa | 1.10 | 0.035 | | |
| | X(3) = Concrete compressive strength, $f_c$’ | 1.08 | 0.15 | Lognormal | [64] |
| Geometry | X(4) = Diameter of circular section, $D$ | 1.00 | 0.005 | Lognormal | [61] |
| | X(5) = Width of rectangular section, $B$ | 1.00 | 0.009 | Lognormal | [61] |
| | X(6) = Height of rectangular section, $H$ | 1.00 | 0.009 | Lognormal | [61] |
| | X(7) = Thickness of steel tube, $t$ | 0.99 | 0.025 | Lognormal | [61] |
| Load | X(8) = Dead load, $D_n$ | 1.00 | 0.10 | Normal | [69, 70] |
| | X(9) = Live load, $L_n$ for AISC 360-16 | 1.00 | 0.25 | Gumbel | [69, 72] |
| | $L_n$ for EC 4 and AZNZS 2327 | 0.60 | 0.35 | Gumbel | [70, 74, 75] |
| Model error | X(10) = $ME$ | Table 5 | Table 5 | Lognormal | |

Table 7. Load and partial resistance factors

| Load and resistance factors | | AISC 360-16 | EC 4 | ASNZS 2327 |
|---|---|---|---|---|
| Load factor $\gamma$ | Dead load $\gamma_D$ | 1.2 | 1.35 | 1.2 |
| | Dead load $\gamma_L$ | 1.6 | 1.5 | 1.5 |
| Partial resistance factor $\phi$ | Steel | 0.75 | 1.0 | 0.9 |
| | Concrete | 0.75 | 0.67 | 0.65 |

Table 8. Number of samples required in MCS with a CoV of 5%

| Reliability index $\beta$ | 3 | 3.5 | 4 | 4.5 | 5.0 | 5.5 | 6.0 |
|---|---|---|---|---|---|---|---|
| Failure probability $P_f$ | 0.0013 | $2.33\times10^{-4}$ | $3.17\times10^{-5}$ | $3.40\times10^{-6}$ | $2.87\times10^{-7}$ | $1.90\times10^{-8}$ | $3.40\times10^{-6}$ |
| No. of sample $N$ | $2.96\times10^{5}$ | $1.72\times10^{6}$ | $1.26\times10^{7}$ | $1.18\times10^{8}$ | $1.40\times10^{9}$ | $2.11\times10^{10}$ | $4.05\times10^{11}$ |
| Computational time (s)* | 3.0 | 16.2 | 122.7 | 2000.0 | - | - | - |

* Using a HP EliteBook X360 1030 G2 Notebook (i7 CPU and 16 GB RAM).

Table 9. Reliability index $\beta$ of considered codes within and beyond code limits

| Column type | Reliability index $\beta$ | AISC 360-16 | | EC 4 | | ASNZS 2327 | |
|---|---|---|---|---|---|---|---|
| | | Within | Beyond | Within | Beyond | Within | Beyond |
| Circular column (CC) | Min | 3.06 | 3.05 | 3.90 | 3.63 | 3.82 | 3.71 |
| | Max | 4.59 | 4.53 | 5.31 | 5.90 | 5.22 | 5.24 |
| | Mean | 3.66 | 3.62 | 4.42 | 4.57 | 4.34 | 4.38 |
| | CoV | 0.08 | 0.07 | 0.07 | 0.11 | 0.06 | 0.07 |
| Rectangular column (RC) | Min | 3.11 | 3.06 | 3.47 | 3.24 | 3.56 | 3.40 |
| | Max | 3.97 | 3.81 | 4.87 | 5.35 | 4.79 | 4.82 |
| | Mean | 3.43 | 3.36 | 4.00 | 4.15 | 4.04 | 4.09 |
| | CoV | 0.06 | 0.04 | 0.08 | 0.11 | 0.06 | 0.07 |
| Circular beam-column (CB) | Min | 2.42 | 2.18 | 2.89 | 2.83 | 2.57 | 2.53 |
| | Max | 3.43 | 3.60 | 3.99 | 4.12 | 4.33 | 4.40 |
| | Mean | 2.99 | 2.96 | 3.49 | 3.65 | 3.64 | 3.70 |
| | CoV | 0.06 | 0.06 | 0.08 | 0.08 | 0.09 | 0.09 |
| Rectangular beam-column (RB) | Min | 2.84 | 2.72 | 2.79 | 2.77 | 2.62 | 2.47 |
| | Max | 3.50 | 3.63 | 3.75 | 3.92 | 4.20 | 4.22 |
| | Mean | 3.06 | 3.00 | 3.34 | 3.49 | 3.57 | 3.65 |
| | CoV | 0.06 | 0.04 | 0.07 | 0.07 | 0.09 | 0.10 |

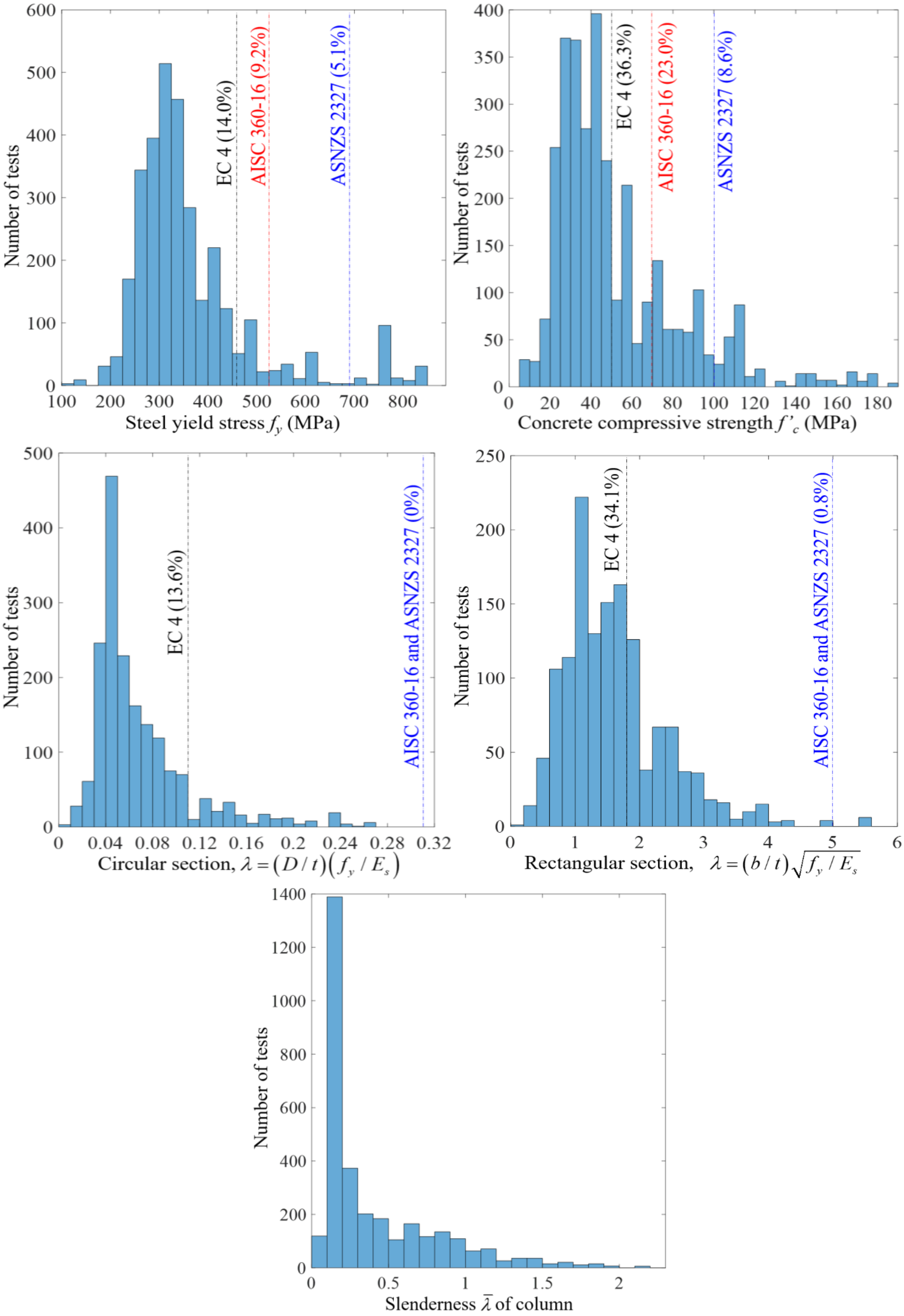


Fig. 1. Histogram of test database

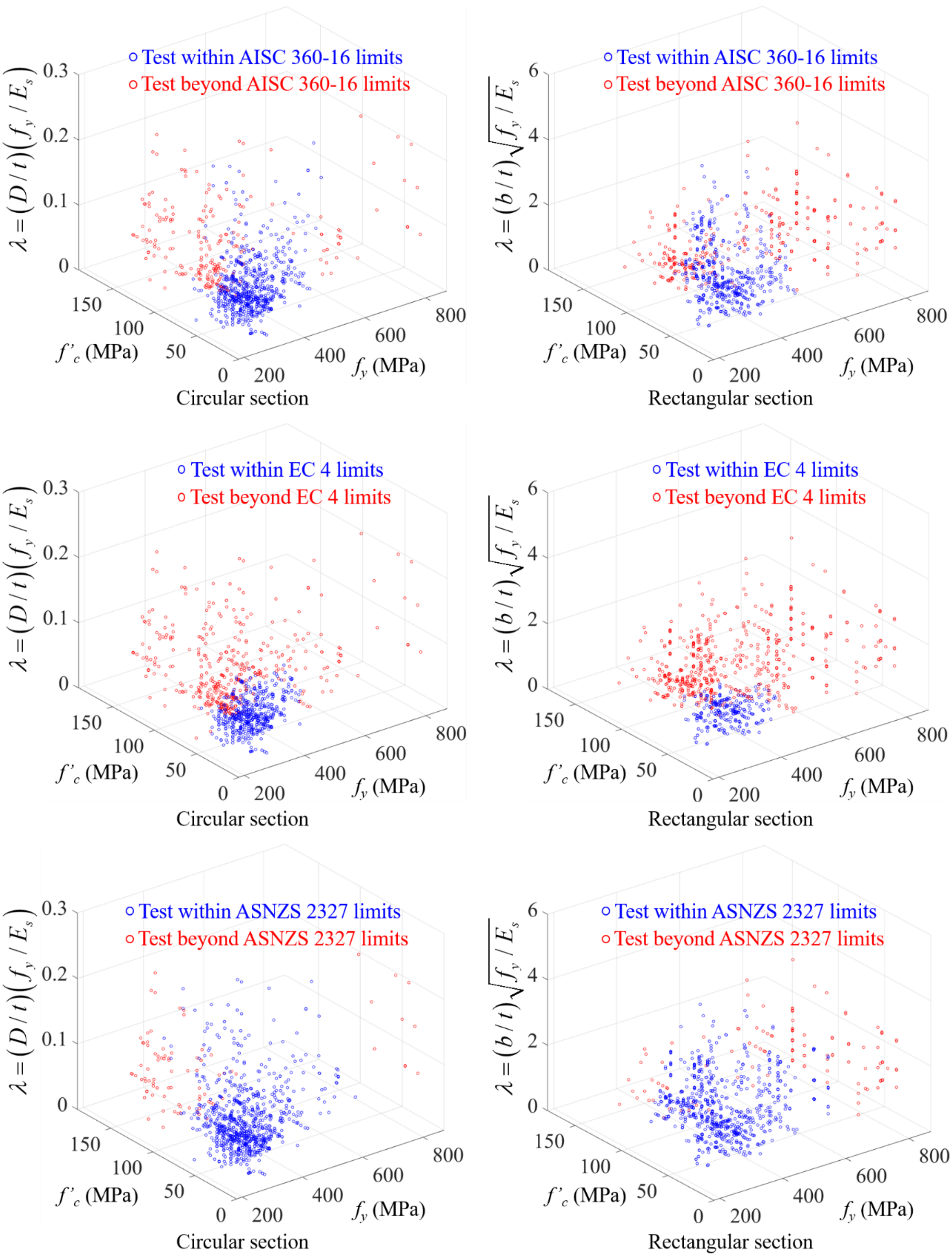


Fig. 2. Distribution of tests within and beyond code limits

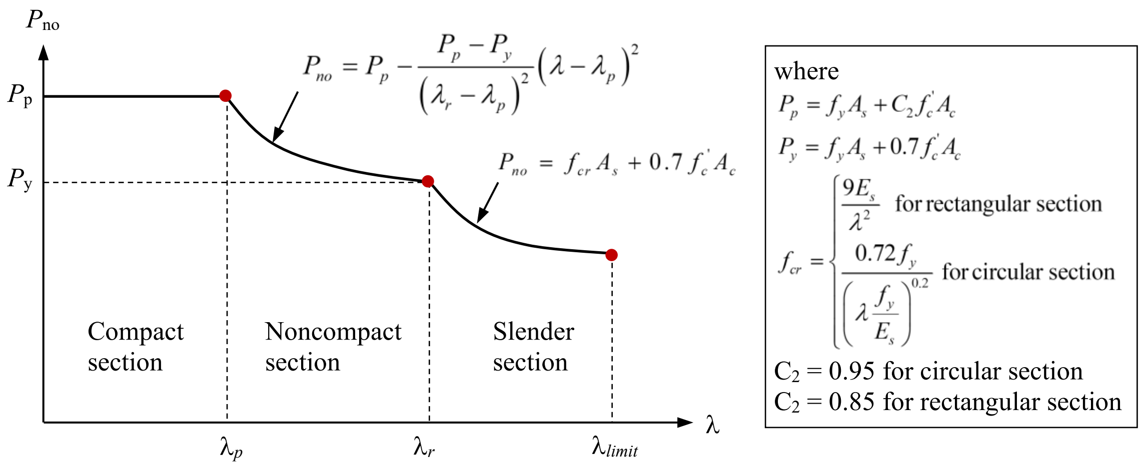


Fig. 3. Variation of nominal section strength ($P_{no}$) with respect to section slenderness ($\lambda$)

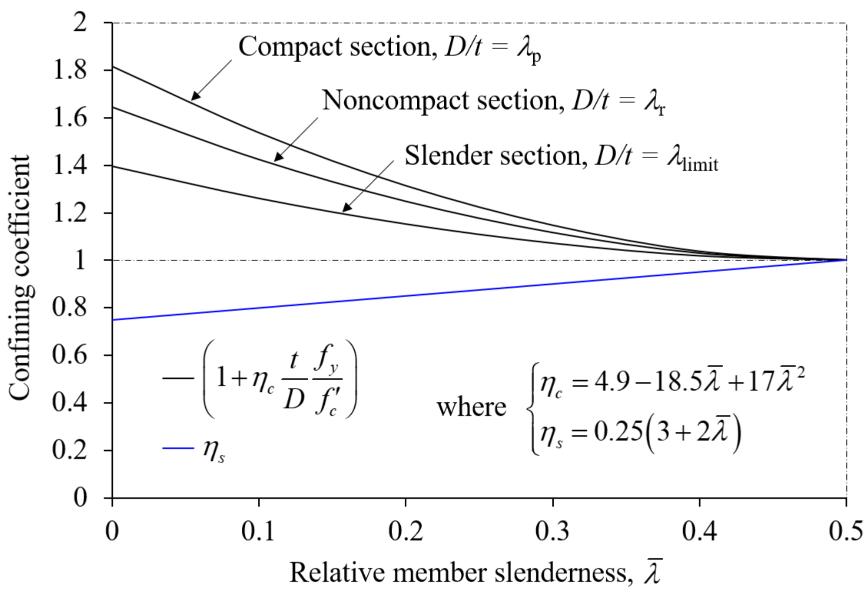


Fig. 4. Confining coefficient with respect to relative member slenderness

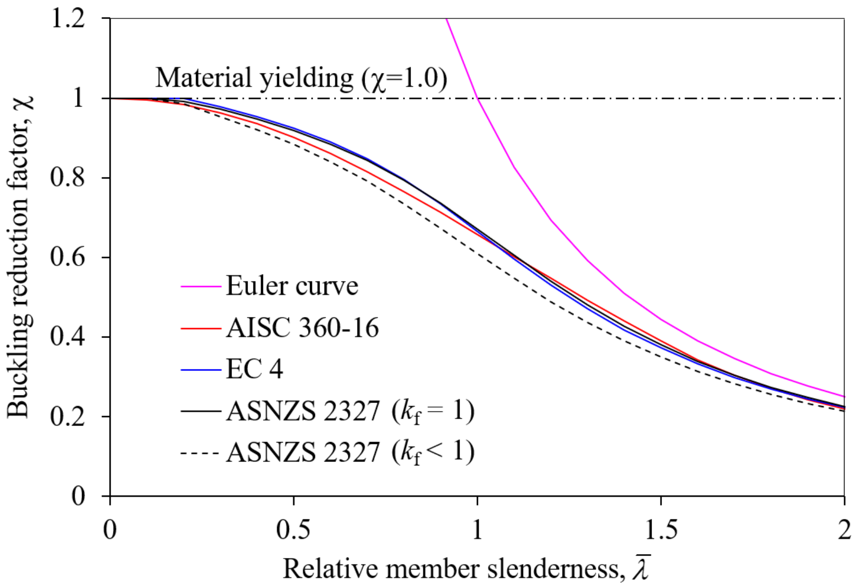


Fig. 5. Column curves from three considered design codes

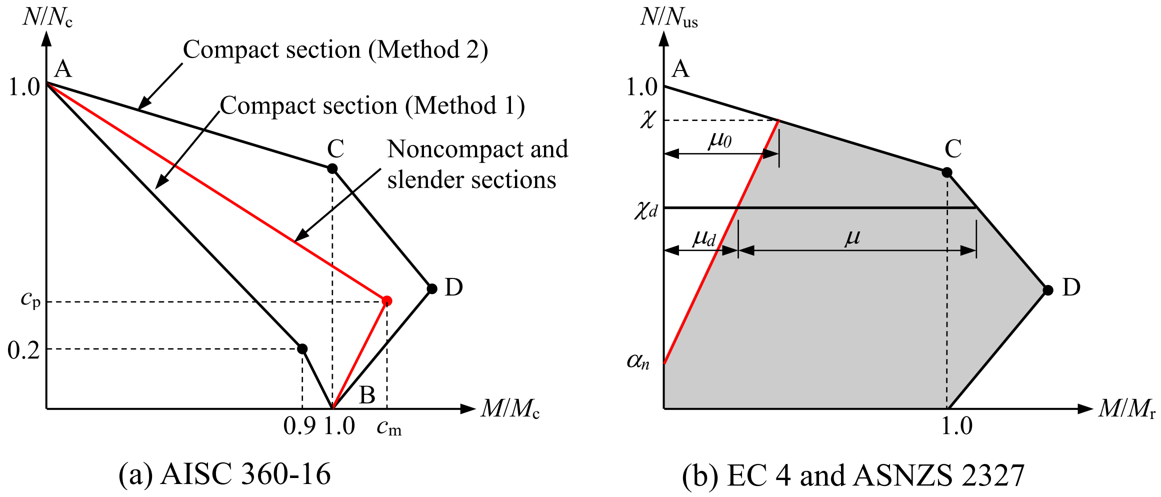


Fig. 6. Non-dimensional N-M interaction diagram of eccentric columns

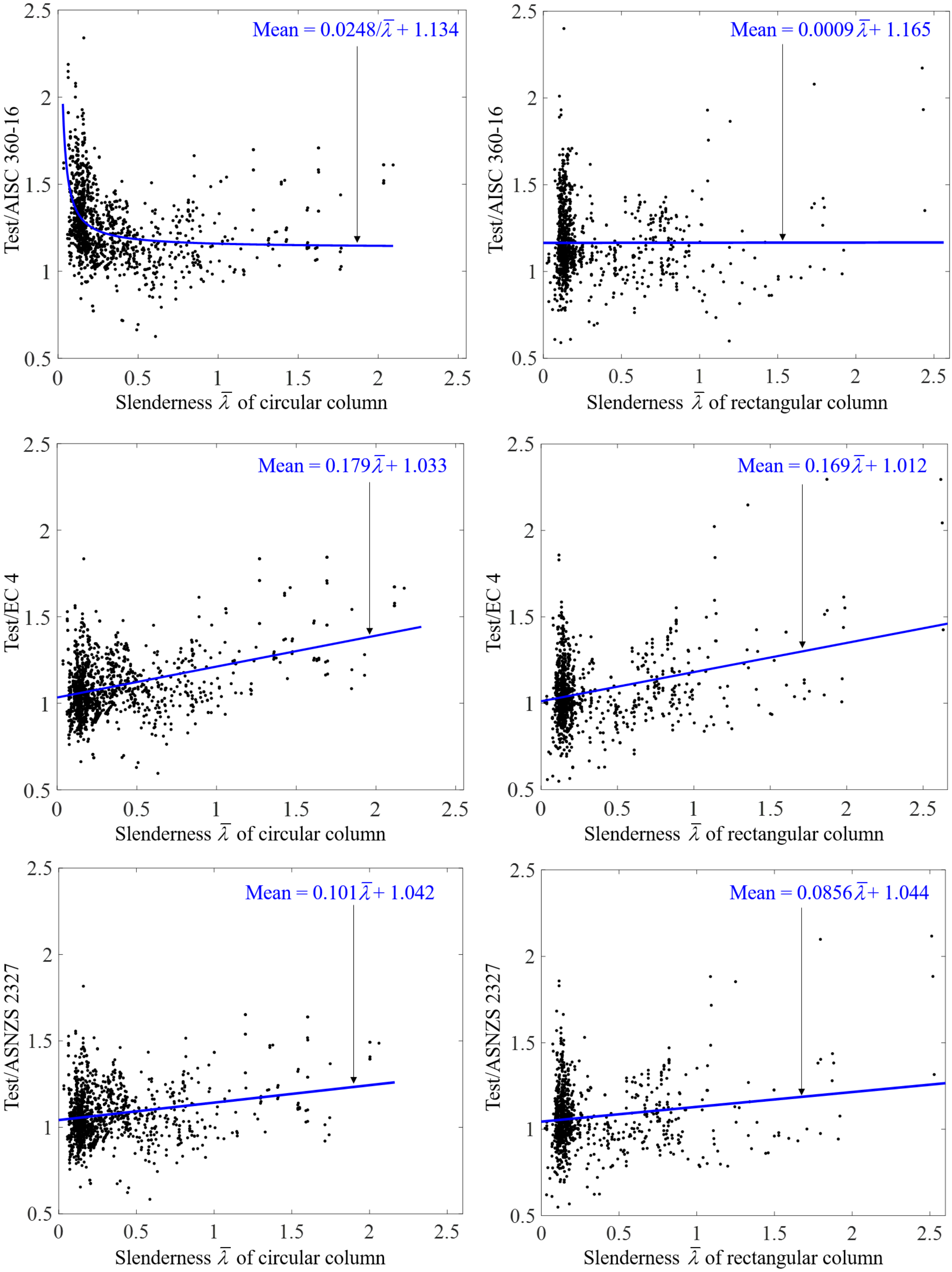


Fig. 7. Test-to-code prediction with respect to the member slenderness of concentric columns

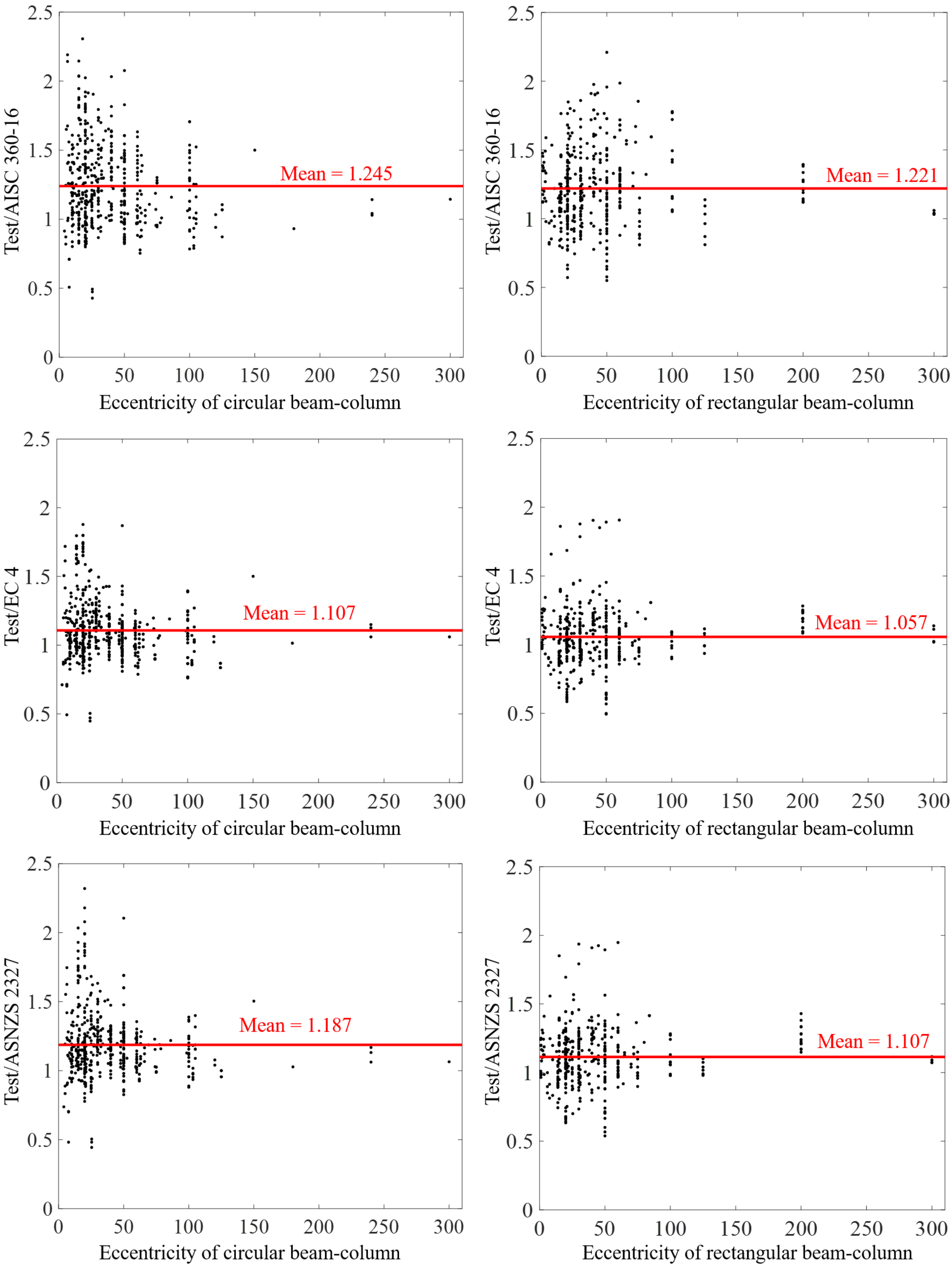


Fig. 8. Test-to-code prediction with respect to the eccentricity of eccentric columns

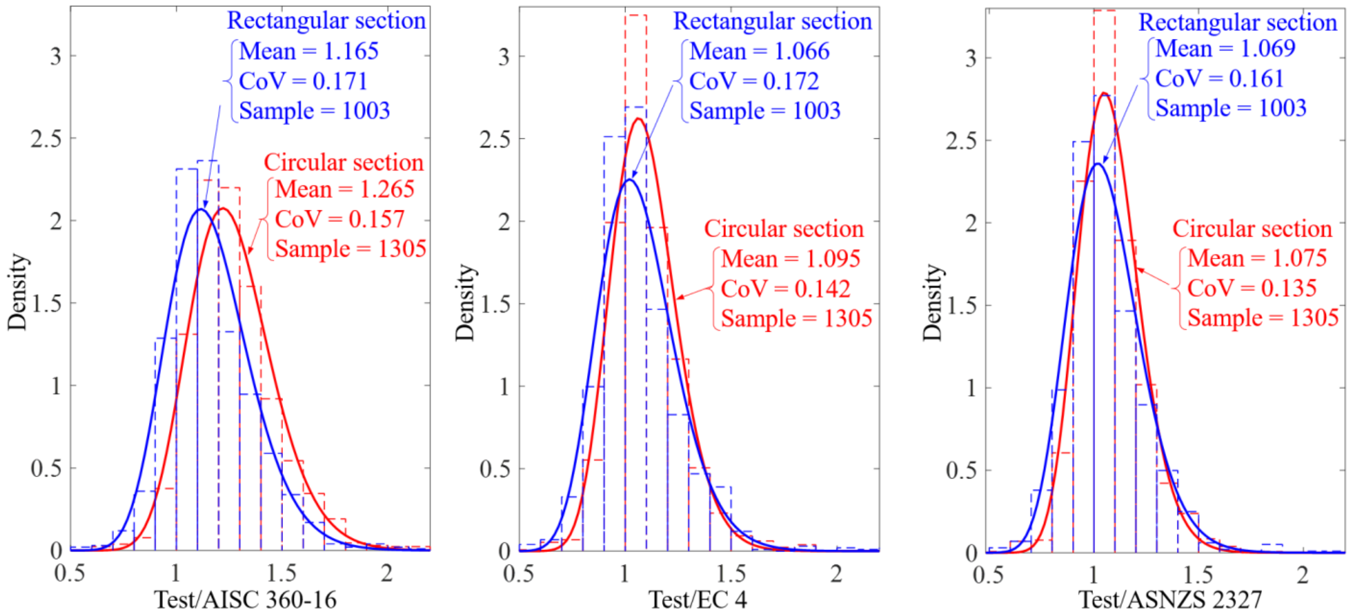


Fig. 9. Histogram of test-to-prediction ratio of concentric columns

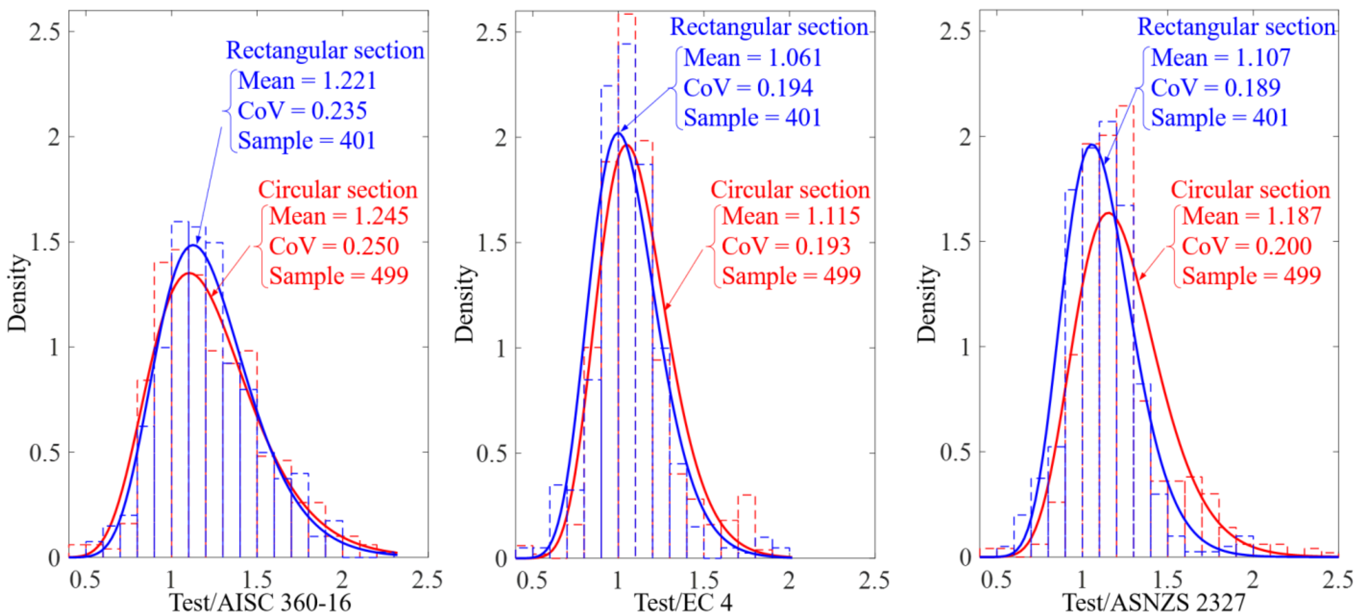


Fig. 10. Histogram of test-to-prediction ratio of eccentric columns

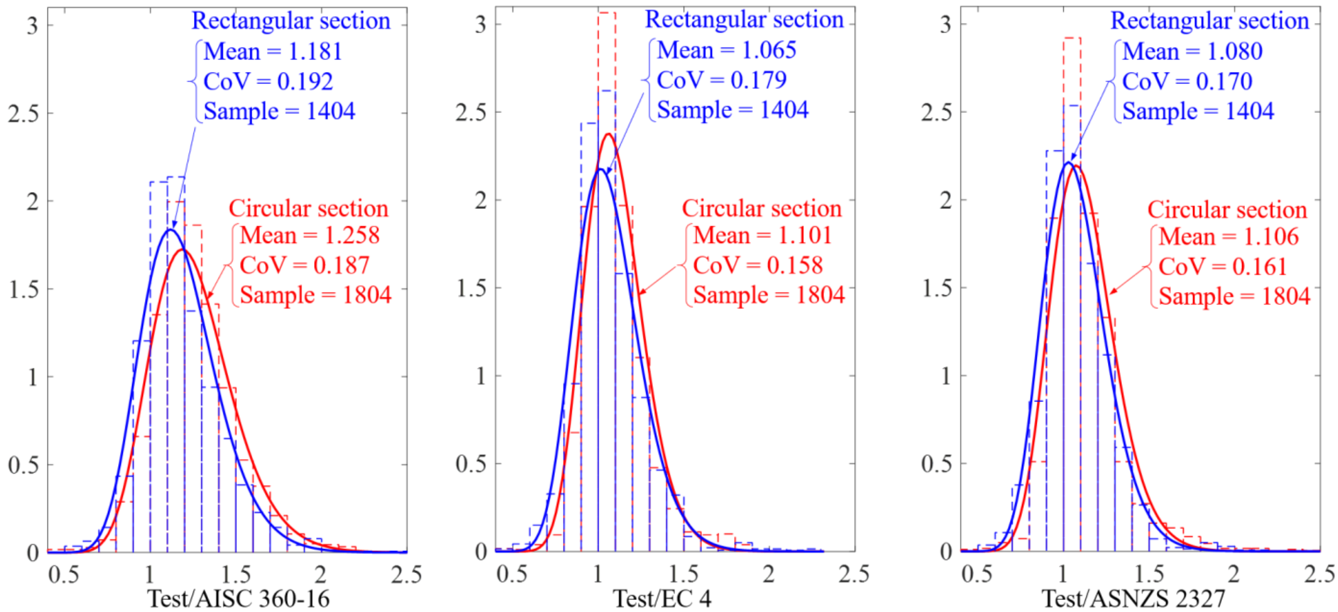


Fig. 11. Histogram of test-to-prediction ratio of all tests

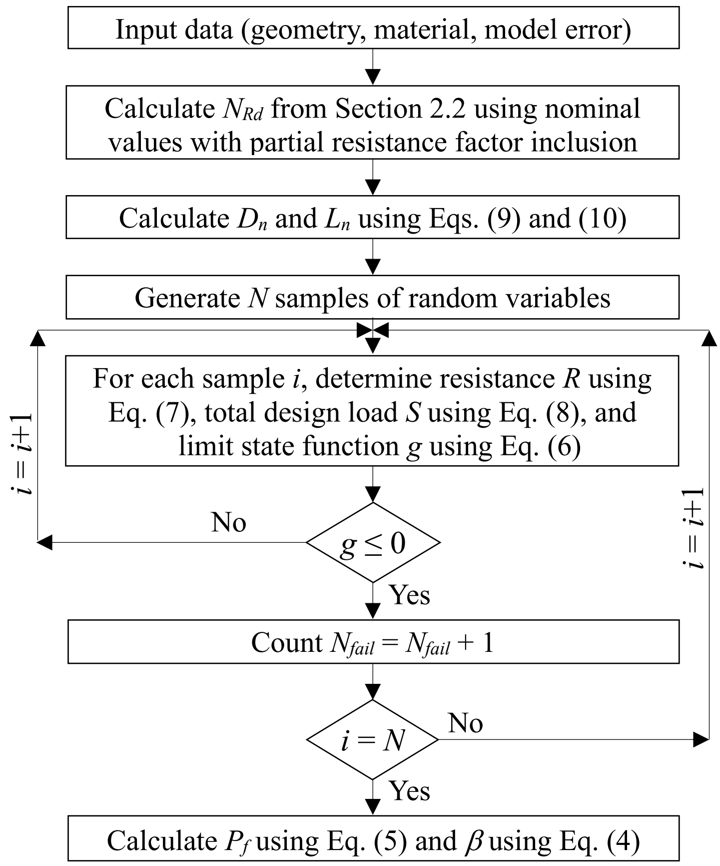


Fig. 12. Flowchart of MCS

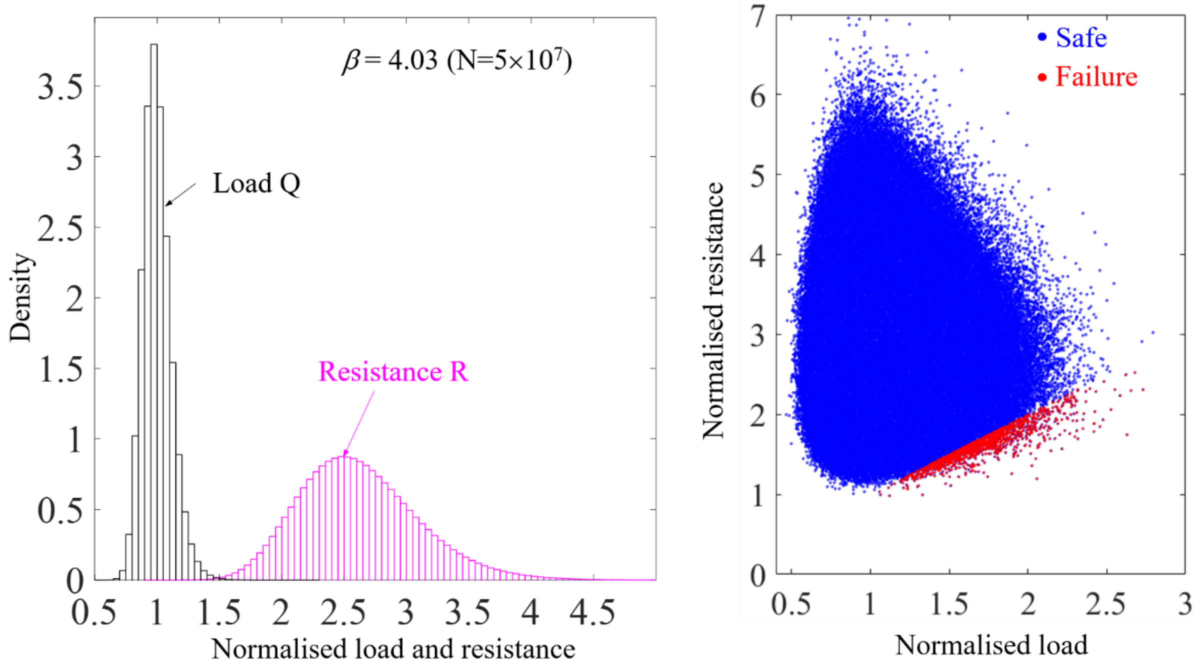


(a) Histograms and distribution of samples from MCS

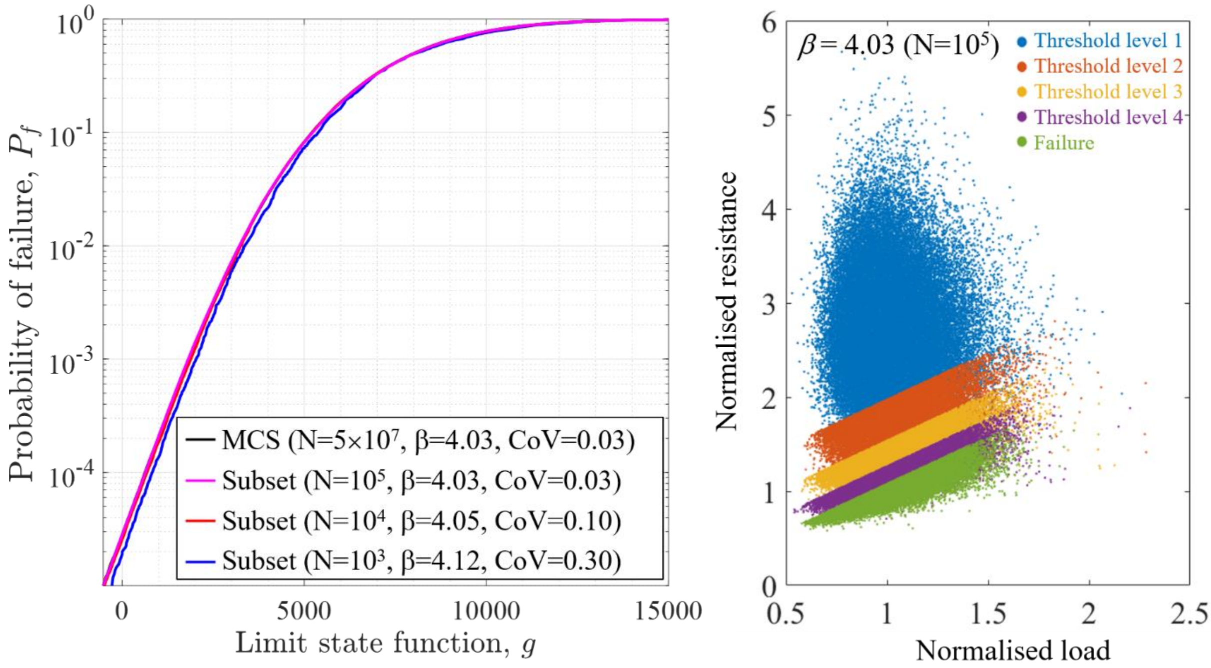


(b) Prediction of failure probability and distribution of samples from subset simulation

Fig. 13. MCS and subset simulation of a typical square stub column designed by ASNZS

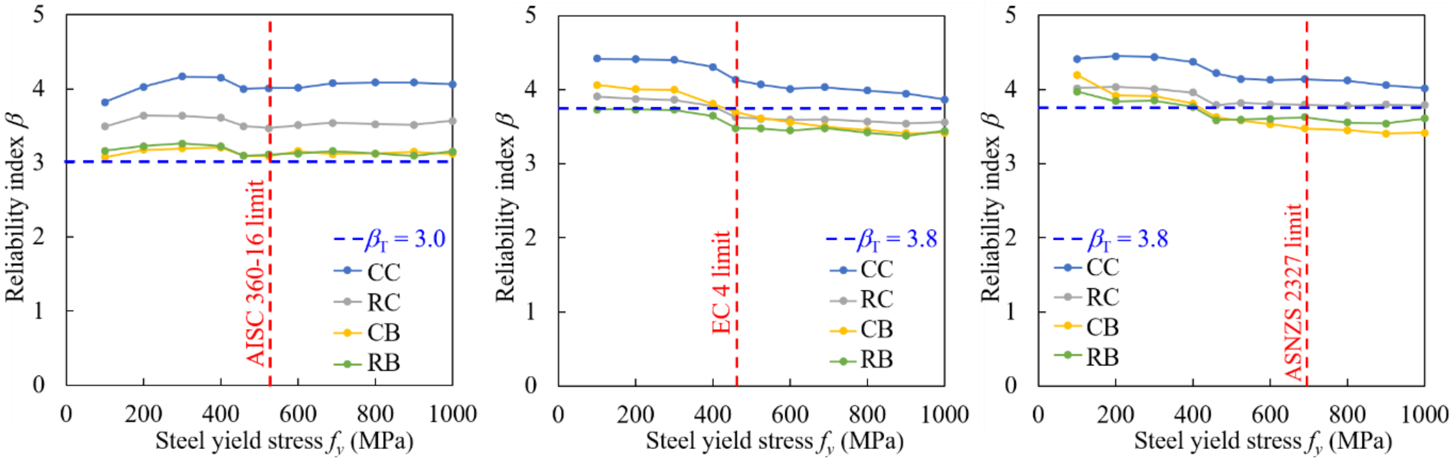


(a) AISC 360-16 (b) EC 4 (c) ASNZS 2327

Fig. 14. Effect of $f_y$ on the reliability index of three codes

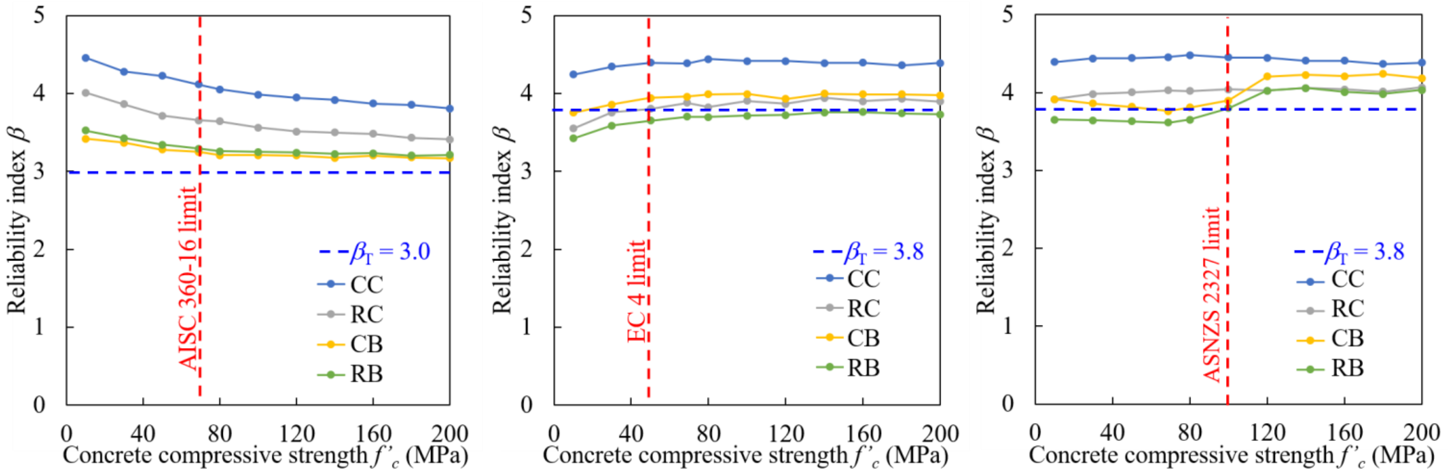


(a) AISC 360-16 (b) EC 4 (c) ASNZS 2327

Fig. 15. Effect of $f_c$' on the reliability index of three codes

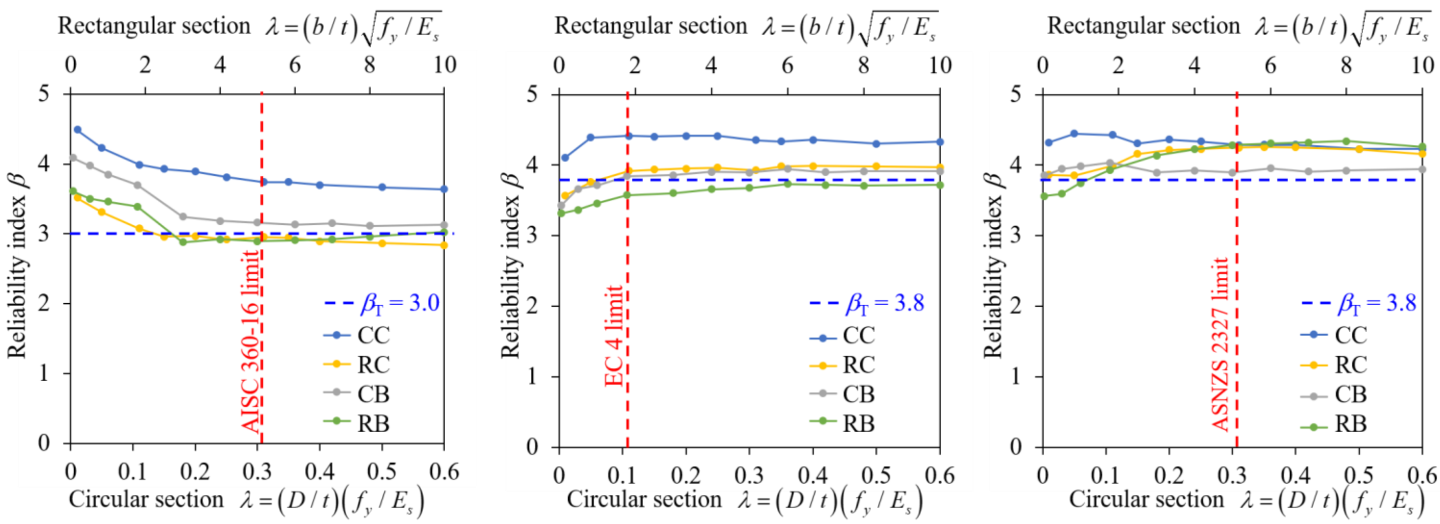


(a) AISC 360-16 (b) EC 4 (c) ASNZS 2327

Fig. 16. Effect of $\lambda$ on the reliability index of three codes

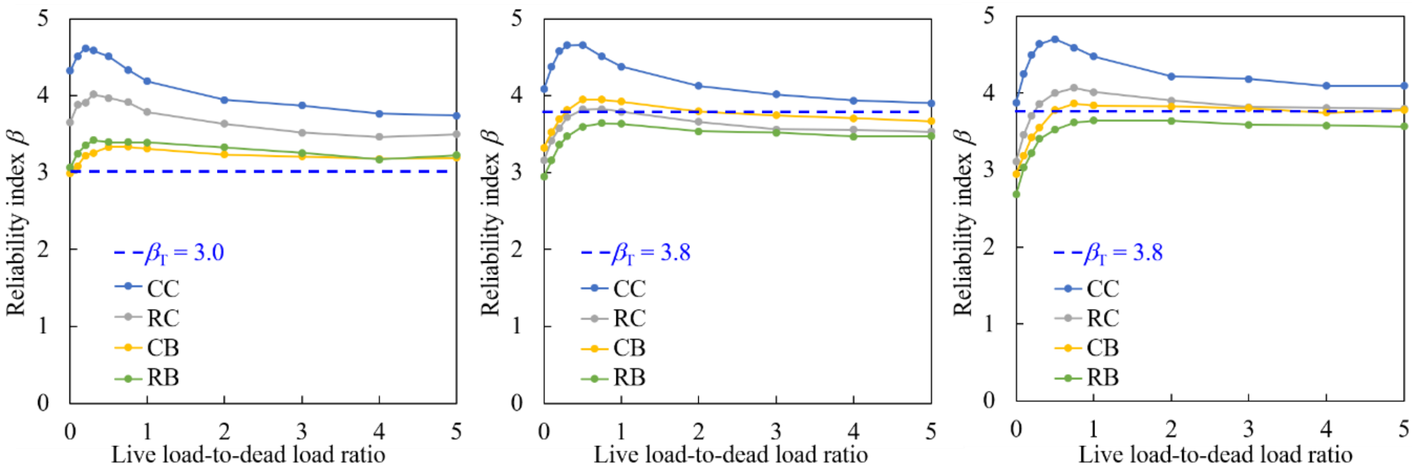


(a) AISC 360-16 (b) EC 4 (c) ASNZS 2327

Fig. 17. Effect of live load-to-dead load ratio on the reliability index of three codes